



Lysine-36 of *Drosophila* histone H3.3 supports adult longevity

John C. Brown ^{1,†} Benjamin D. McMichael,^{1,2,†} Vasudha Vandadi,^{1,†} Aadit Mukherjee,² Harmony R. Salzler,^{1,*} A. Gregory Matera ^{1,2,3,4,*}

¹Integrative Program for Biological and Genome Sciences, University of North Carolina, Chapel Hill, NC 27599, USA

²Department of Biology, University of North Carolina, Chapel Hill, NC 27599, USA

³Department of Genetics, University of North Carolina, Chapel Hill, NC 27599, USA

⁴RNA Discovery Center, Lineberger Comprehensive Cancer Center, University of North Carolina, Chapel Hill, NC 27599, USA

*Corresponding author: IBGS Program, University of North Carolina, 3352 Genome Sciences Bldg, Chapel Hill, NC 27599, USA. Email: hsalzler@email.unc.edu;

*Corresponding author: IBGS Program, University of North Carolina, 3352 Genome Sciences Bldg, Chapel Hill, NC 27599, USA. Email: matera@unc.edu (A.G.M.)

[†]These authors contributed equally to this work.

Aging is a multifactorial process that disturbs homeostasis, increases disease susceptibility, and ultimately results in death. Although the definitive set of molecular mechanisms responsible for aging remain to be discovered, epigenetic change over time is proving to be a promising piece of the puzzle. Several post-translational histone modifications have been linked to the maintenance of longevity. Here, we focus on lysine-36 of the replication-independent histone protein, H3.3 (H3.3K36). To interrogate the role of this residue in *Drosophila* developmental gene regulation, we generated a lysine-to-arginine mutant that blocks the activity of its cognate-modifying enzymes. We found that an *H3.3B*^{K36R} mutation causes a significant reduction in adult lifespan, accompanied by dysregulation of the genomic and transcriptomic architecture. Transgenic co-expression of wild-type *H3.3B* completely rescues the longevity defect. Because H3.3 is known to accumulate in nondividing tissues, we carried out transcriptome profiling of young vs aged adult fly heads. The data show that loss of H3.3K36 results in age-dependent misexpression of NF- κ B and other innate immune target genes, as well as defects in silencing of heterochromatin. We propose H3.3K36 maintains the postmitotic epigenomic landscape, supporting longevity by regulating both pericentric and telomeric retrotransposons and by suppressing aberrant immune signaling.

Keywords: histone variant; post-transcriptional modification; PTMs; aging; senescence; telomeres; retrotransposition; gene expression; innate immunity; heterochromatin

Introduction

Eukaryotic genomes are condensed in the nucleus of each cell as chromatin, a dynamic blend of histones, proteins, and DNA. Nucleosomes, the fundamental unit of chromatin, comprise ~150 base pairs of DNA wrapped around an octamer of histones. Nucleosomes not only allow organisms to compress and store vast amounts of genetic information, but they also serve as steric barriers to a variety of DNA-templated processes (Lorch *et al.* 1987; Ransom *et al.* 2010; Bell *et al.* 2011). Accordingly, molecular mechanisms have evolved to alter and regulate genome accessibility. Included among these mechanisms for chromatin remodeling are the covalent post-translational modification (PTM) of histones and the incorporation of histone variants (Talbert and Henikoff 2010; Bannister and Kouzarides 2011; Clapier *et al.* 2017).

Histone tail residues sustain a remarkable diversity of PTMs, including methylation, acetylation, ubiquitylation, sumoylation, and phosphorylation (Li *et al.* 2007; Rothbart and Strahl 2014). Histone PTMs are hypothesized to alter local chromatin states via direct and indirect methods. For example, lysine acetylation alters chromatin directly by neutralizing positively charged lysine residues and weakening electrostatic interactions between

histones and DNA (Eberharter and Becker 2002). In contrast, other modifications function through the recruitment of effector proteins (Rothbart and Strahl 2014).

The incorporation of variant histones further increases regulatory complexity. In *Drosophila*, the histone gene complex (*HisC*) encodes all five canonical histone proteins. It is comprised by a cluster of ~100 tandemly repeated, 5 kb repeat units that encode H2A, H2B, H3, H4, as well as the linker histone H1. Canonical (replication-dependent) histones are synthesized and incorporated into chromatin during S phase of the cell cycle. Variant (replication-independent) histones are encoded by genes located outside of *HisC* and are synthesized and incorporated independently of DNA replication. Variant histones typically contain a few amino acid residue changes from their canonical counterparts, which can alter their PTMs, stability within the nucleosome, and interactions with other chromatin components (Talbert and Henikoff 2010).

Here, we focus on lysine-36 of the replication-independent histone, H3.3, and its role in regulating lifespan. H3.3 differs from the canonical H3 (H3.2) by four amino acids (Elsässer *et al.* 2010). These few differences enable a number of unique protein–protein interactions and PTM preferences (McKittrick *et al.* 2004; Filipescu

et al. 2013). Ascomycete genomes, including budding yeast and other fungi, possess only one noncentromeric H3 protein, which is orthologous to metazoan H3.3. In budding yeast, mutation of either H3K36 or Set2, the enzyme that catalyzes mono-, di-, and trimethylation of H3K36, causes replicative aging defects (Sen et al. 2015). In nematodes, inactivation of met-1, the Set2 ortholog, also decreases lifespan, whereas loss of H3.3 decreases the lifespan of long-lived *Caenorhabditis elegans* mutants (Ni et al. 2012; Pu et al. 2015; Piazzesi et al. 2016). Although these results suggest that H3.3K36 plays a conserved role in metazoan lifespan regulation, direct genetic tests of a role for this histone residue in aging have been lacking.

To investigate the function of H3.3K36 in *Drosophila* gene expression regulation, we previously generated a lysine-to-arginine mutant, H3.3B^{K36R} (Salzler et al. 2023). Here, we show that an H3.3B^{K36R} mutation (expressed in an H3.3A^{null} background) causes age-dependent dysregulation of the transcriptome, resulting in a significantly reduced adult lifespan. This longevity defect can be rescued by ectopic expression of a wild-type H3.3B transgene. We also show that loss of H3.3K36 histones causes overexpression of NF- κ B target genes in the adult brain, a disruption in several key aging-related metabolic processes, and progressive deterioration in silencing of heterochromatin. Indeed, we found clear evidence for age-dependent upregulation of repetitive elements, particularly LTR-type retrotransposons. Remarkably, the expression of LINE-like elements specifically involved in telomere maintenance was decreased. These findings lead us to propose that H3.3K36 supports longevity not only by promoting cellular homeostasis but also by suppressing the activity of transposable elements (TEs) and innate immune response genes in the adult brain.

Materials and methods

Fly husbandry and genetics

We generated H3.3^{K36R} mutants by combining a K36R missense mutation at H3.3B (Salzler et al. 2023) and combining it with an H3.3A^{2 \times 1} null mutation (Sakai et al. 2009) in *trans* to the Df(2L)Bsc110 deficiency chromosome (H3.3A Δ). Experimental progeny obtained from crosses were screened using both H3.3A^{null} and H3.3^{K36R}. Animals were obtained by negative selection for the CyO, twGFP chromosome (see Supplementary Fig. S1 for details). The H3.3A^{2 \times 1} and Df(2L)Bsc110 alleles were obtained from Bloomington *Drosophila* Stock Center (#68240, #8835). The H3.3 rescue transgene was created in an earlier study (Penke et al. 2018). Crosses were carried out in cages sealed with grape juice agar plates with supplemental yeast paste. Plates were replaced daily and GFP-negative larvae were sorted into vials of cornmeal-molasses food. Experimental flies were raised at 25°C, and all experiments were performed at 25°C unless otherwise noted.

Adult lifespan assays

To assess longevity, parental stocks were mated on grape juice agar plates and larvae were sorted into vials of molasses food. For each replicate, 50 larvae were sorted into fresh food vials (total of four to six replicates per genotype) and the fraction (%) of animals that pupated and eclosed was calculated. The mean and standard deviation for each genotype were plotted with GraphPad Prism software. Following eclosion, male and female flies were kept in separate vials. Animals that eclosed within 48 h of each other were considered the same age in subsequent assays. To measure adult lifespans, each vial contained twenty or fewer flies to avoid crowding and was incubated on its side to reduce accidental deaths from animals getting stuck in the food.

Dead flies were removed and survivors flipped into fresh food every 2–3 days to prevent death due to poor conditions. Survivors were recounted and recorded after each flip. Flies that were killed or escaped during the experiment were removed from the count.

Fly head RNA extraction and RNA-sequencing

H3.3^{K36R} and H3.3^{null} animals were generated as above and were separated into groups based on the date of eclosion. Flies that eclosed within 48 h of each other were considered an age cohort. Young cohorts (0–2 days posteclosion) were processed without further aging, whereas old cohorts were processed after three weeks (21–25 days posteclosion). Heads were removed from the rest of the carcass and total RNA was extracted. For each biological replicate, 10–25 flies were anesthetized and placed in a 15 mL tube. The tube was submerged in liquid nitrogen for 5–10 s and then vortexed for 5–10 s to separate heads from carcasses. This process was repeated for a total of five times before pouring the contents of the tube into a set of stacked sieves (Cole-Parmer, 3"-Diameter Sieve, Full Height Stainless Steel, No. 25 on top of Cole-Parmer, 3"-Diameter Sieve, Full Height Stainless Steel, No. 40). Fly heads were recovered from the bottom sieve and either stored at –80°C or immediately used for RNA extraction. Fly heads were crushed in the TRIzol reagent (Thermo Fisher), and RNA was purified with the RNA clean and concentrator-5 kit (Zymo research), and equivalent amounts of RNA per replicate were used for cDNA library construction. Total (Ribo-minus) RNA-seq libraries, six (three male, three female) replicates per genotype, were prepared using a Universal RNA-seq library kit with NuQuant (Tecan). Sequencing was performed on a NovaSeq 6000SP (Illumina) producing 100 nt, paired-end reads.

RNA-Seq analysis and datasets

Raw and processed RNA-seq data were deposited to Gene Expression Omnibus (GEO) under accession GSE244389. Quality control was performed with FastQC, ver. fastqc/0.11.7 (Andrews 2010), and reads were aligned using STAR (Dobin et al. 2013) to genome build dm6. Aligned reads were counted with featureCounts (Liao et al. 2014) and differential gene expression analysis was performed with DESeq2 (v1.34.0) (Love et al. 2014). One outlying sample was removed from the downstream analysis. Standard DESeq2 protocols were used to determine the statistical significance of differential gene expression analysis. The so-called “interaction model” (design = sex + age + genotype + age:genotype) takes into account changes in the effect size and direction between the two conditions and the genotypes (Love et al. 2014). Therefore this model places greater statistical weight on gene expression differences that result from the interaction between genotype and condition. Coding resources used for data processing can be found using the following DOI: <https://doi.org/10.5281/zenodo.10553305>.

Gene names, annotations, genome sequence, and a wealth of other pertinent information used in this study were obtained from FlyBase (Gramates et al. 2022). Gene ontology (GO) analyses were performed using g:Profiler (Reimand et al. 2007; Aleksander et al. 2023). Differential transposon analysis was performed using Tetrascripts (Jin et al. 2015). The statistical model used in this case included sex and genotype, as we chose to compare old mutants to old control animals.

Assignment of differentially expressed genes to chromatin states

Files containing Chromatin State information for larval BG3 cells, as defined previously (Kharchenko et al. 2011), were downloaded

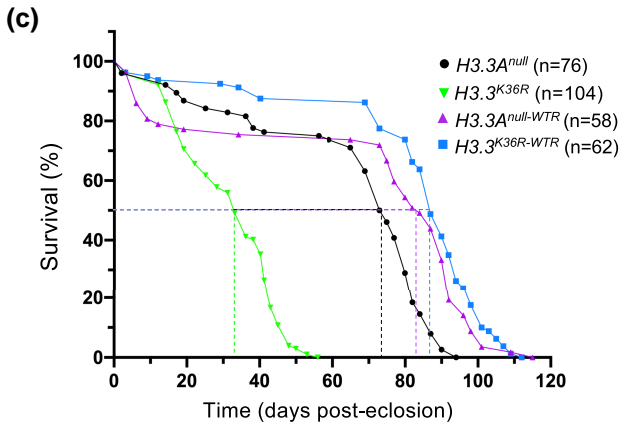
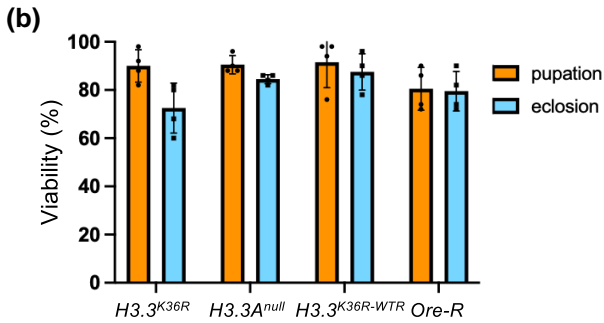
(a)

$$H3.3A^{null} = \frac{+}{+}; \frac{H3.3A^{2x1}}{Df(2L)Bsc110}; \frac{+}{+}$$

$$H3.3^{K36R} = \frac{H3.3BK36R}{H3.3BK36R}; \frac{H3.3A^{2x1}}{Df(2L)Bsc110}; \frac{+}{+}$$

$$H3.3A^{null-WTR} = \frac{+}{+}; \frac{H3.3A^{2x1}}{Df(2L)Bsc110}; \frac{tg:H3.3B^{WT}}{+}$$

$$H3.3^{K36R-WTR} = \frac{H3.3BK36R}{H3.3BK36R}; \frac{H3.3A^{2x1}}{Df(2L)Bsc110}; \frac{tg:H3.3B^{WT}}{+}$$



	H3.3A ^{null}	H3.3 ^{K36R}	H3.3A ^{null-WTR}	H3.3 ^{K36R-WTR}
H3.3A ^{null}	---	< 10 ⁻⁶ ****	< 4.2 × 10 ⁻³ *	---
H3.3 ^{K36R}	< 10 ⁻⁶ ****	---	---	< 10 ⁻⁶ ****
H3.3A ^{null-WTR}	< 4.2 × 10 ⁻³ *	---	---	ns
H3.3 ^{K36R-WTR}	---	< 10 ⁻⁶ ****	ns	---

Fig. 1. H3.3^{K36R} mutation reduces adult lifespan relative to H3.3A^{null} and wild-type rescue (WTR) controls. a) Detailed genotypes for H3.3A^{null}, H3.3^{K36R}, H3.3A^{null-WTR}, and H3.3^{K36R-WTR} animals. The notation *tg:H3.3B^{WT}* corresponds to the rescue transgene. b) Developmental viability assay. For each genotype, pupation and eclosion frequencies (%) were calculated and plotted (50 larvae per biological replicate vial). The mean and SD of these percentages are shown. Oregon-R (Ore-R) was used as an additional control. c) Adult longevity assays for H3.3A^{null} and H3.3A^{null-WTR} controls, and for H3.3^{K36R} and H3.3^{K36R-WTR} flies. Median lifespan was determined (dotted lines) by identifying the day at which 50% of the animals survived. Statistical comparison of survival curves using Gehan-Breslow-Wilcoxon tests are presented in the accompanying table. A Bonferroni correction for multiple comparisons was employed, resulting in the following adjusted significance values: *P < 0.0125, **P < 0.0025, ***P < 2.5 × 10⁻⁴, ****P < 2.5 × 10⁻⁵.

from the modENCODE website. Gene interval coordinates for transcription-start and -end sites (TSSs and TESs) were intersected with the Chromatin State files using BEDTools (Quinlan and Hall 2010) to assign genes to a given state if they were covered by greater than 50% over its length. Those wherein no State exceeded 50% coverage were labeled as mixed. Genes were binned by state and plotted by log₂-fold change values determined by DESeq2 (Love et al. 2014) using the noninteraction model.

Position effect variegation experiments

Position effect variegation (PEV) reporter lines were obtained from the Bloomington *Drosophila* Stock Center: 118E-12, stock #84015; 39C-62, #44261; 118E-16, #84106; 8-M114, #84095; 8-M76, #84096; and 8-M112, #84093. These PEV lines carry a variegating *hsp70::miniwhite* insertion (Wallrath and Elgin 1995). To assess the role of H3.3K36 in heterochromatin spreading, PEV males with an H3.3A^{2x1}/CyO 2nd chromosome were crossed to *yw*, H3.3BK36R; *Df(Bsc110)/CyO*, *twGFP* (H3.3BK36R) or *yw*; *Df(Bsc110)/CyO*, *twGFP* (H3.3AA) virgin females. Straight-winged male flies were age-matched, and flies that eclosed within 96 h of each other were grouped together. Images were taken on the following day, so the flies were 1–5 days posteclosion.

Western blotting

Protein lysates from whole wandering third instar (WL3) larvae (ten animals per replicate) were obtained by homogenization with a micropestle in SUTEB buffer [1% SDS, 8 M urea, 10 mM EDTA (pH 8.0), and 5% β-mercaptoethanol, with 1:20 Halt protease inhibitor cocktail (Thermo Fisher Scientific, no. 78429)]. Chromatin was further disrupted by sonication with a Bioruptor Pico (Diagenode).

Samples were electrophoresed on 4 to 15% Mini-PROTEAN TGX Stain-Free protein gels (Bio-Rad, #4568084) for 60 min at 100 V. Western blotting was performed using the Bio-Rad Trans Blot Turbo transfer system using the provided buffer (Bio-Rad, no. 10026938) onto a nitrocellulose membrane at 1.3A/25 V for 7 min. Membranes were blocked at RT in 5% milk in TBS-T (Tris buffered saline, Tween 20). Primary antibody incubation was overnight at 4°C in TBS-T with 5% milk with one of the following antibodies: polyclonal rabbit anti-H4 pan acetyl (1:1000; Activemotif, no. 39925) or polyclonal rabbit anti-H3 (Abcam, #1791). For each primary antibody, an anti-rabbit secondary (Sigma-Aldrich, no. 12-348) was used at 1:5000.

Blots were incubated with a chemiluminescent detection reagent (Amersham ECL Prime Western Blotting Detection Reagents, GE Healthcare, no. RPN2236) and imaged on an Amersham Imager 600 (GE Healthcare). Between primary antibody antibodies, blots were stripped, rinsed in TBS-T, and incubated with a detection reagent to verify the removal of antibody before reprobing. Relative band intensity ratios were calculated using NIH ImageJ. Briefly, a box of equal size and dimension was drawn around each band, and integrated density (IntDen) inside the box was recorded. For each blot, a ratio of H4ac/H3 IntDen was calculated per sample lane. In addition, a normalized value for each mutant genotype was calculated by dividing the mutant ratio by that of the control H3.3A^{null} genotype. Lysates from yellow-white (*yw*) wild-type control animals, along with 12xH3.2K36R mutants. Quantification of the data from 12xH3.2K36R mutants was not used in the graphical comparison due to differences in overall histone gene number (each of

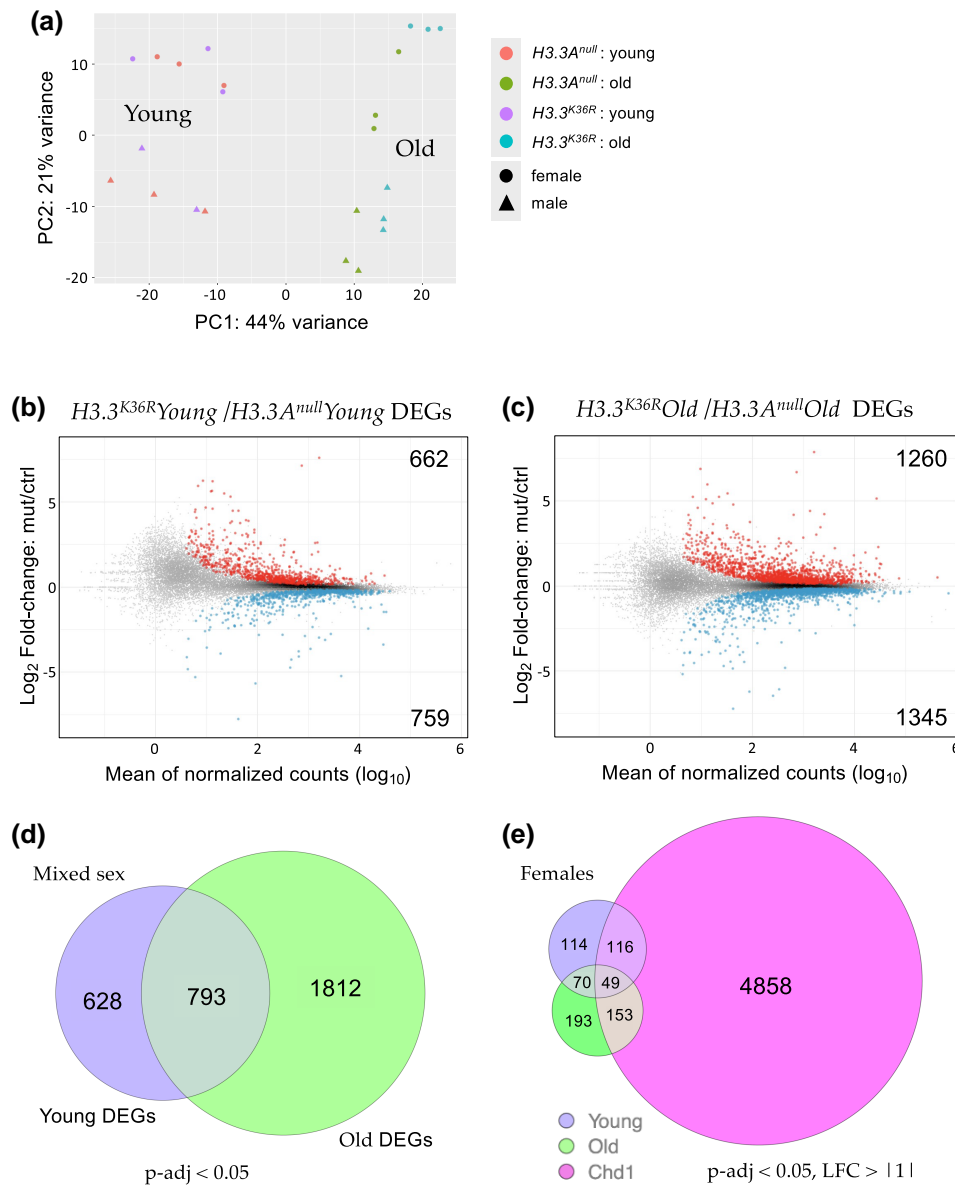


Fig. 2. Transcriptomic profiling of young and old adult fly brains. a) PCA of young (0–2 d posteclosion) and old (21–25 d) $H3.3A^{null}$ and $H3.3^{K36R}$ fly heads, labeled by sex. b) M/A plot comparing gene expression from mixed sex $H3.3^{K36R}$ and $H3.3A^{null}$ young fly heads. Differentially shaded dots represent DEGs that were significantly (adjusted P-value, $P\text{-adj} < 0.05$) up- (red, above midline) or downregulated (blue, below). The number of DEGs in each direction is shown in the upper and lower corners. c) M/A plot of mixed sex $H3.3^{K36R}$ vs $H3.3A^{null}$ transcripts from old adults. Labeling and significance as per panel (b). d) Venn diagram comparing overall number of DEGs ($P\text{-adj} < 0.05$) between $H3.3A^{null}$ and $H3.3^{K36R}$ genotypes, young and old mixed sex fly heads. e) Venn diagram of DEGs ($P\text{-adj} < 0.05$ and \log_2 -fold change $\geq |1|$) from female $H3.3^{K36R}$ (young or old) vs aged (20 d) female $Chd1$ fly heads. Data for $Chd1$ provided by Schoberleitner et al. (2021).

the other genotypes contain $200\times$ copies of the replication-dependent histone genes).

Results

$H3.3^{K36R}$ causes an adult lifespan defect

Drosophila histone H3.3 protein is encoded by two genes, $H3.3A$ on the second chromosome and $H3.3B$ on the X chromosome (Akhmanova et al. 1995). We previously engineered a missense mutation in $H3.3B$ ($H3.3B^{K36R}$) using Cas9-mediated homologous DNA repair, for details see (Salzler et al. 2023). By combining the $H3.3B^{K36R}$ mutation with deletion of $H3.3A$ ($H3.3A^{null}$), we generated $H3.3^{K36R}$ animals that completely lack $H3.3K36$ (Fig. 1a, Supplementary Fig. 1). We also utilized an $H3.3B^{WT}$ transgene inserted onto the third chromosome (Penke et al. 2018) to generate

$H3.3A^{null-WTR}$ and $H3.3^{K36R-WTR}$ (wild-type rescue) flies (Fig. 1a, Supplementary Fig. 1). As shown in Fig. 1b, the majority of $H3.3A^{null}$, $H3.3^{K36R}$, and $H3.3^{K36R-WTR}$ animals complete development and eclose as adults at similar frequencies to a wild-type Oregon R (Ore-R) control. Thus, arginine substitution of $H3.3K36$ has no significant effect on organismal viability.

To understand the role that this residue might play in longevity, we carried out adult lifespan assays. We measured the lifespan of $H3.3^{K36R}$ mutants and compared the results to those obtained for $H3.3A^{null}$ control animals (Fig. 1c, graph). Note that the $H3.3A^{null}$ genotype has a small, but significant decrease in median lifespan by comparison to an Ore-R wild-type strain (Supplementary Fig. 2). As defined by the number of days (posteclosion) at which 50% of the animals survived, the $K36R$ mutation has a pronounced and highly significant effect on adult lifespan (Fig. 1c, table).

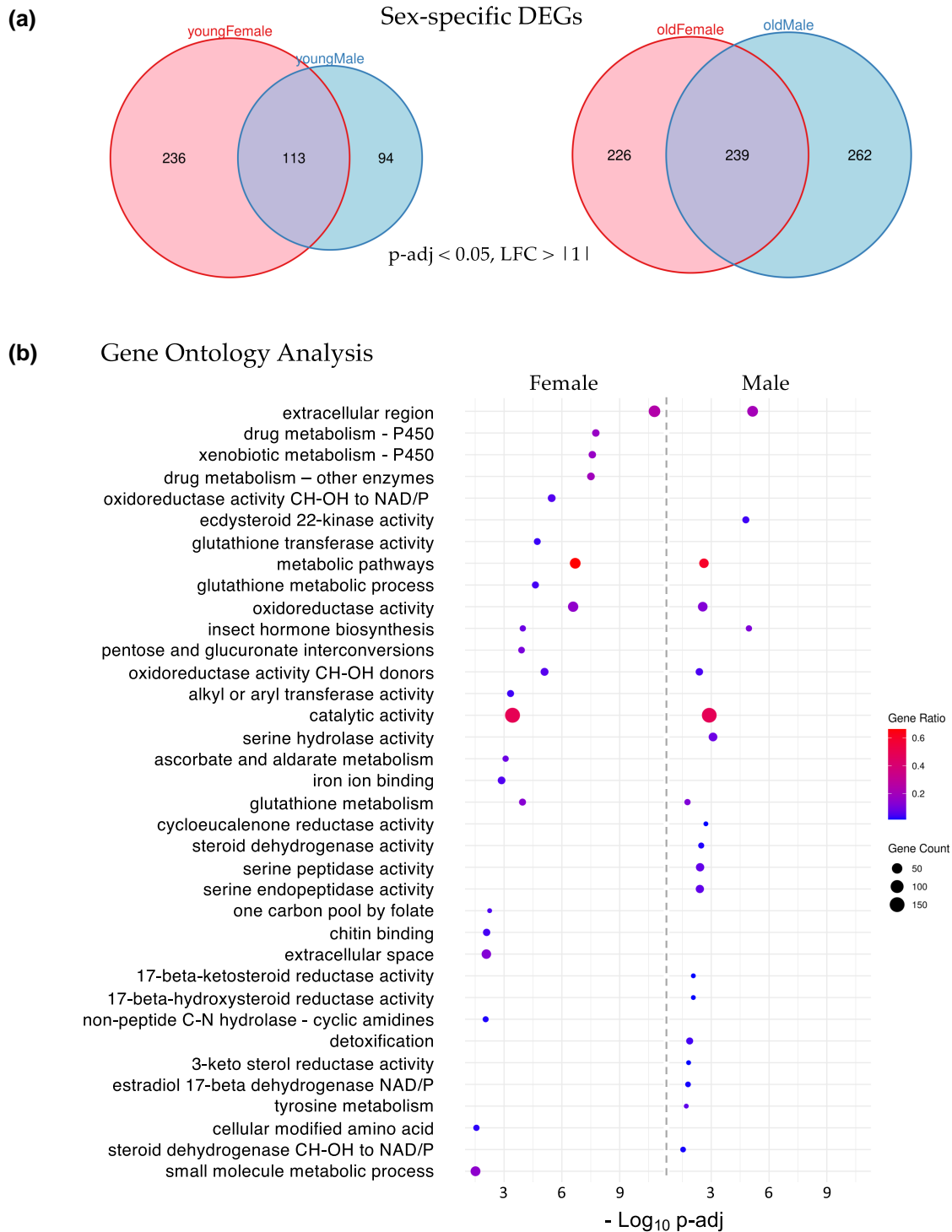


Fig. 3. Sex-specific analysis of significant DEGs. a) Venn diagrams of age- and sex-specific DEGs ($P\text{-adj} < 0.05$ and $LFC > |1|$) between $H3.3^{K36R}$ vs $H3.3^{A^{null}}$ fly heads. Left diagram compares DEGs in young female with young male fly heads (0–2 d posteclosion), and right diagram compares DEGs in old female with old male fly heads (21–25 d). b) GO analysis of the DEGs identified in panel (a) (old female and old male). The size of each dot is proportional to the number of genes contained within a given ontology term (gene count), and the fraction of those genes scoring significantly (gene ratio) is represented using a heatmap. Adjusted P -values ($-\log_{10}$ transformed) for each GO term were calculated and plotted separately for both females and males.

Furthermore, ectopic expression of wild-type H3.3 protein fully rescued this defect. That is, the median survival time of $H3.3^{K36R}$ mutants was roughly 33 days posteclosion, whereas that of $H3.3^{K36R-WTR}$ control animals was 87 days (Fig. 1c, graph). To minimize the potential effects of genetic background on longevity, we employed isogenic second chromosomes and crossed closely related strains together to produce the experimental genotypes (Supplementary Fig. 1). Rescue

of the shortened lifespan by expression of a wild-type $H3.3B$ transgene strongly suggests that the longevity defect is due to the $H3.3B^{K36R}$ mutation. Thus, we conclude that mutation of H3.3 lysine-36 causes a substantial reduction in adult lifespan. Consistent with previous studies showing that H3.3 is essential for lifespan extension in nematodes (Piazzi et al. 2016), this work shows that lysine-36 plays a direct role in this process.

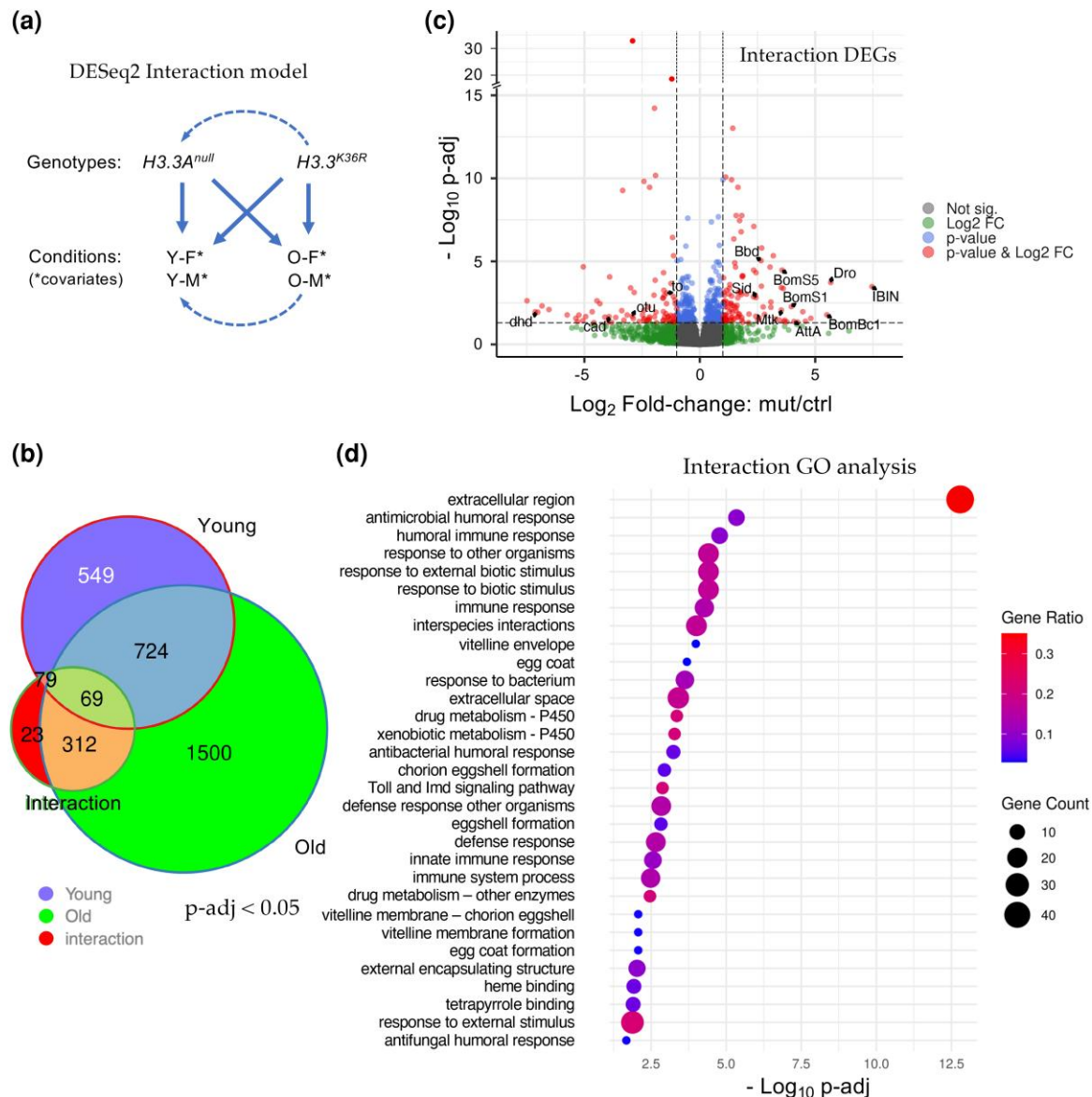


Fig. 4. Analysis of the interaction between age and genotype in old and young fly heads. a) Graphical representation of the DESeq2 model including interaction terms (design = sex + age + genotype + age:genotype). Solid arrows represent genotype:condition terms, dotted arrows illustrate how the model sets reference levels. b) Venn diagram of DEGs ($P\text{-adj} < 0.05$) in young $H3.3^{K36R}$ vs $H3.3A^{null}$ (0–2 d posteclosion) and old $H3.3^{K36R}$ vs $H3.3A^{null}$ fly heads (21–25 d), compared to those identified using the interaction model (age:genotype). c) Volcano plot of RNA-Seq data obtained using the interaction model. Dotted lines represent significance cutoffs for adjusted P-value and \log_2 -fold change. Dots represent individual genes, color coded according to the key at right. d) GO analysis of DEGs ($P\text{-adj} < 0.05$ and $LFC > |1|$) that were determined using the interaction model. Adjusted P-values ($-\log_{10}$ transformed) for each GO term were calculated and plotted. The size of each dot is proportional to the number of genes contained within a given ontology term (gene count), and the fraction of those genes scoring significantly (gene ratio) is represented using a heatmap.

Gene expression analysis in young vs old fly heads from $H3.3^{K36R}$ mutants and controls

Organismal lifespan is influenced by multiple interconnected factors, many of which are unknown, and most of which are poorly understood (Zhang et al. 2015; Garschall and Flatt 2018; Aron et al. 2022). Although cellular senescence is a natural and beneficial process in certain contexts, the accumulation of senescent cells over time is thought to contribute to aging and age-related diseases (Childs et al. 2015). Despite their relatively short lifespan, many fundamental mechanisms underlying aging are conserved between fruit flies and humans, making *Drosophila* a valuable model for studying senescence-related processes. The brain of the adult fly is composed primarily of diploid postmitotic cells

that rely on histone variant-specific assembly mechanisms for nucleosome turnover (Konev et al. 2007). Indeed, H3.3 is reportedly enriched in the adult fly brain, and its deposition increases with age (Schoberleitner et al. 2021). Thus, brain cells should be particularly sensitive to the potential effects of a histone H3.3 missense mutation.

To gain insight into mechanisms by which H3.3K36 might influence age-dependent regulation of gene expression, we carried out transcriptome profiling of young vs old fly heads. As detailed in the Materials and Methods, adult head RNA was extracted from six replicates (three male and three female) of each age:genotype pair (young and old $H3.3A^{null}$ and young and old $H3.3^{K36R}$ animals). Libraries were prepared from total, Ribo-minus RNA samples and subjected to 100nt, paired-end RNA-sequencing (RNA-seq) using

standard procedures (see Methods for details). Principle component analysis (PCA) of the dataset (Fig. 2a) shows that the samples segregate primarily on the basis of age (PC1) and sex (PC2). Furthermore, the old adult samples can be distinguished by genotype-specific differences (Fig. 2a).

In order to identify differentially expressed genes (DEGs), we plotted the \log_2 -fold change ($H3.3^{K36R}/H3.3A^{null}$) for each transcript, vs the mean of normalized counts for that transcript. Among the younger flies, we found that there were 1,421 genes (662 up, 759 down) that were differentially expressed (P -adj < 0.05) in the mutant vs control samples (Fig. 2b). A similar M/A plot comparing the older mutant and control animals showed that there were 2,605 DEGs (1260 up and 1345 down, Fig. 2c). Deposition of H3.3 protein in adult heads has been shown to increase with age from ~17% of total H3 in newly-eclosed animals to ~34% in 20–25 day old flies like the ones used here (Schoberleitner et al. 2021). Consistent with this finding, we identified nearly twice as many DEGs in the older dataset, 793 of which overlapped with those in the younger animals (Fig. 2d).

To maximize the chances of capturing H3.3-specific effects, we focused our attention on DEGs identified in the older age group, and compared them to an RNA-seq dataset prepared from similarly-aged female *Chd1* (*chromodomain-helicase-DNA binding protein 1*) null mutants, using a separate DESeq2 model using data only from females (Schoberleitner et al. 2021). *Chd1* protein is part of a histone chaperone complex that functions together with Hira (Histone regulator A) to specifically deposit H3.3 into chromatin in the adult brain and other postmitotic tissues (Konev et al. 2007). *Chd1* null animals display a very similar adult longevity phenotype to $H3.3^{K36R}$ (K36R) mutants (Schoberleitner et al. 2021). Differential expression analysis of *Chd1* null animals identified roughly 12,000 DEGs (P -adj < 0.05). Unsurprisingly, most of the previously identified (young + old) K36R DEGs were contained within this large set (Supplementary Fig. 3a). We therefore applied more stringent cut-offs (P -adj < 0.05, $\log_2 FC > |1|$) to highlight the genes with the greatest magnitude changes in all three groups and found that the overlap was greatly reduced. For this more stringent comparison, we also restricted it to our female K36R datasets, because the *Chd1* DEGs were derived from female-only fly heads (Fig. 2e). Strikingly, the degree of overlap between the old K36R and *Chd1* DEGs went from roughly 84% to around 43% (Supplementary Fig. 3b). Moreover, all of the non-*Chd1* overlapping transcripts in the old female K36R dataset remained above the higher stringency threshold (Fig. 2e). Thus, the K36-specific DEGs, generally represented larger magnitude changes.

Interestingly, the female K36R fly head transcriptome appears to be affected earlier, and disrupted to a greater extent, than that of the male (Fig. 3a). Parsing out the longevity data in Fig. 1 by sex revealed that female K36R mutants had a median lifespan of around 30 d, compared to 40 d for males (Supplementary Fig. 4). Functional enrichment analysis of the old female DEGs produced a number of senescence-associated GO terms (Ashburner et al. 2000; Gene Ontology Consortium et al. 2023). These include genes involved in metabolic pathways that include cytochrome P450 and other enzymes, such as oxidoreductases (Fig. 3b). In contrast, GO analysis of old male K36R mutants identified detoxification factors, serine peptidases, and ecdysteroid insect hormone enzymes (Fig. 3b). Interestingly, brain extracellular region proteins were identified in both sexes. This category of genes is among the hallmarks of the senescence-associated secretory phenotype (SASP), which has been implicated as a driver of numerous age-related disorders (Naylor et al. 2013; Mavrogonatou et al. 2023; Mebratu et al. 2023). Another prominent GO term category,

identified in both males and females, centers around the oxidation and transport of glutathione (Fig. 3b). In studies from nematodes to mice, glutathione has been broadly implicated in brain disorders and cellular senescence (Liu et al. 2004; Gusarov et al. 2021; Iskusnykh et al. 2022). Altogether, these data support the view that H3.3K36 is important for maintaining cellular homeostasis in the adult brain.

A statistical interaction model highlights defects in innate immune signaling

Though informative, our comparison to the *Chd1* RNA-seq dataset (Schoberleitner et al. 2021) and our original DESeq2 model were unable to take into account the effects of both age and sex. We therefore wanted to design an experiment to interrogate the differential effects that age and sex have on $H3.3^{K36R}$ flies, relative to $H3.3A^{null}$ controls. As shown in Fig. 4a, we used DESeq2 and R to create a multifactorial statistical model with two genotypes ($H3.3^{K36R}$ and $H3.3A^{null}$), four conditions (i.e. with age and sex as covariates), and the interaction between age and genotype (age:genotype). This new model places higher weight on gene expression differences that result from the interaction between genotype and condition, rather than by identifying significant differences within a genotype in two separate conditions (for additional details, see Methods). The interaction model thus accounts for the fact that the control genotype could have a different baseline (Fig. 4a) for each of the various conditions (young and old). Strikingly, the age:genotype interaction model reduced the total number of statistically significant gene expression changes (P -adj < 0.05) from 3,256 down to 483 transcripts (Fig. 4b and Supplementary Table 1). Only 312 out of the 1812 “Old-only” DEGs classified in the previous comparison (Fig. 2d) were found to be significant in the interaction model, and 23 new DEGs were uncovered (Fig. 4b).

A volcano plot of all the genes identified using the age:genotype interaction is shown in Fig. 4c. As illustrated, the distribution of the Interaction DEGs (P -adj < 0.05, LFC > |1|, red dots) was roughly equal between up- and downregulated genes. Notable among the genes whose expression went up are numerous downstream targets of NF- κ B signaling. These include the antimicrobial peptides (AMPs) Drosomycin (Drs), Drosocin (Dro), Attacin A (Atta), Metchnikowin (Mtk), and Bomanins S1, S2, S3, and S5; Bc1, Bc3; T1, T2, T3 (Fig. 4c and Supplementary Table 1). Other well-known immune effectors include IBIN/CG44404, IM4/CG15231, IM14/CG33990, Bbd/CG18067, and SPH93/CG44404. These host defense factors are encoded by well-known antibacterial and antifungal response genes that are targeted by the Toll and IMD signaling pathways (Lindsay et al. 2018; Hanson et al. 2021). Indeed, the NF- κ B ortholog dorsal (*dl*) is itself among the genes that are differentially upregulated in the mutants (Supplementary Table 1).

Among the genes that were significantly reduced in expression are several notable transcription factors, including ovarian tumor (*otu*/CG12743), and caudal (*cad*/CG1759). *Cad* and *otu* are negative regulators of immune (IMD) signaling that, in the adult animal, have been implicated in the maintenance of homeostasis (Ryu et al. 2004, 2008; Ji et al. 2019). Thus, not only are the downstream targets of NF- κ B upregulated, but genes involved in dampening or turning off these pathways are also downregulated. Another indicator of a runaway immune response in the brains of aging K36R mutants is highlighted by a 5-fold upregulation of the *Stress-induced DNase* gene, *Sid*/CG9989 (Supplementary Table 1). *Sid* protein is highly induced by bacterial infection and is thought to protect cells from the toxic effects of excess nucleic acids that are released during a vigorous immune challenge (Seong et al. 2014).

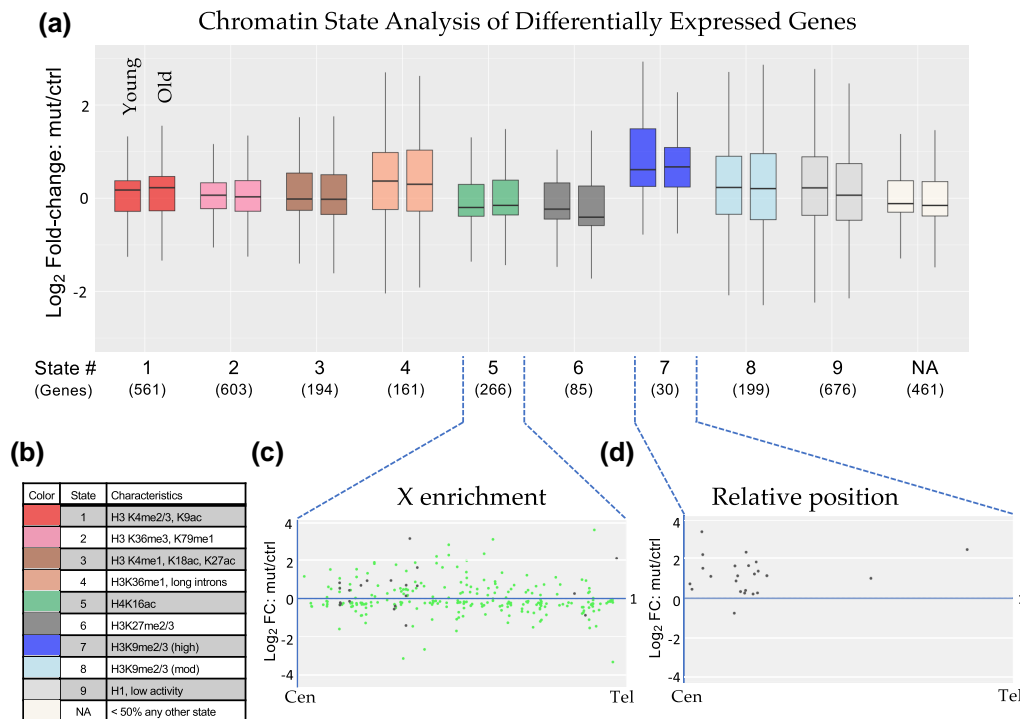


Fig. 5. Chromatin state analysis of DEGs. a) The combined set of DEGs (adjusted P -value < 0.05) from the noninteraction DESeq2 model for both Young and Old conditions for $H3.3^{K36R}$ mutants relative to $H3.3^{null}$ controls was binned by predominant chromatin state (Kharchenko et al. 2011). Genes were binned to a given state if $> 50\%$ of the gene was marked by that state. The “NA” category was comprised of genes where no state color was $> 50\%$ of gene length (406 genes) or if chromatin states were undetermined when the original chromatin state study was published (55 genes). The mut/ctrl \log_2 -fold change value for binned genes was plotted separately for Young and Old conditions. b) A legend for colors corresponding to each chromatin state depicted in panel (a), with representative histone marks for each state. c) and d) For genes in States 5 and 7, mut/ctrl \log_2 -fold change values for the Old condition were plotted vs relative position along chromosome arms for all chromosomes, from centromere (Cen) to telomere (Tel). For State 5, the X chromosome genes are colored green, and autosomal genes, black.

Consistent with the findings outlined above, GO analysis of the Interaction DEGs (using a more stringent P -adj < 0.05 and LFC $> |1|$ cutoff) identified these and many other genes implicating a hyperactivation of immune response pathways in the absence of an external challenge (Fig. 4d). Although these pathways have been clearly implicated in numerous other studies of senescence and aging, the work here provides the first evidence linking them to H3.3K36-dependent processes in animals (see Discussion).

Age-dependent loss of heterochromatic silencing

Previously, we showed that $H3.3^{K36R}$ mutants eclose at significantly higher frequencies than those that lack both copies of H3.3, strongly suggesting that H3.3K36R protein is incorporated into chromatin and is partially functional (Salzler et al. 2023). Chromatin profiling of wandering third instar wing discs showed that the $H3.3^{K36R}$ mutation had little effect on H3K27me3 levels overall, yet the mutant adults displayed mild homeotic transformations (Salzler et al. 2023). Hence, we were interested in determining which types of chromatin might be affected by loss of H3.3 lysine-36.

Kharchenko and colleagues have classified nine different *Drosophila* chromatin “states” that are based on a wide variety of underlying histone marks and binding factors (Kharchenko et al. 2011). We used genome coordinates, derived from profiling data in BG3 larval brain cells, which have been established for each of these states to carry out an analysis of the genes that were differentially expressed in our K36R mutants. Rather than focusing on a small subset of DEGs whose contribution to the phenotype is uncertain, we broadened this analysis to the union set of young

and old DEGs (Fig. 2d). Genes whose coordinates did not overlap with those of any single chromatin state by at least 50% were binned into a tenth (NA) category.

As shown in Fig. 5a, we plotted the mean \log_2 -fold change over time for the DEGs that fell into each of these ten categories (Chromatin States). The plot on the left within each color grouping measures fold-change between young $H3.3^{K36R}$ mutants vs controls, whereas the plot on the right does the same for the older animals. The color code and brief descriptions of the characteristics for each chromatin state (Kharchenko et al. 2011) are provided in Fig. 5b. Base mean expression levels for DEGs in each state are provided for purposes of comparison (Supplementary Fig. 5a). As illustrated, Chromatin States 1–3, which comprise roughly 30% of the genome and are characterized by “active” marks, are relatively unchanged from young to old animals (Fig. 5a). DEGs in States 4, 7, and 8 are characterized by less active marks and showed the greatest degree of change, increasing substantially over adult lifespan. In contrast, DEGs in States 5 and 6 trended towards lower expression levels over time (Fig. 5a). In male cells, State 5 is characteristic of dosage-compensated genes on the X chromosome (high levels of H4K16ac), and as expected, the DEGs in this category were highly enriched on the X (245/266 genes, see Fig. 5c). By definition, we do not expect these same genes to be hyper-H4K16ac in female cells. Parsing this analysis by sex (Supplementary Fig. 5b), we observed a downward trend in males, consistent with a possible role for H3.3K36 in dosage compensation. However, we also observed a similar trend in females where the chromatin status of this group of genes is unknown (Supplementary Fig. 5b). Thus, the effect on these DEGs was not driven solely by males. State 6 genes are

predominantly marked by H3K27me3 and are likely to be negatively regulated by the Polycomb repressive complex, which has been implicated in aging in *Drosophila* and other species (Siebold *et al.* 2010; Ni *et al.* 2012; Sen *et al.* 2016).

The DEGs in State 7 showed the greatest degree of expression change in young adults as well as in change over time (Fig. 5a). State 7 is characterized by high levels of heterochromatic H3K9me2/3 marks (Fig. 5b). Although there was no single chromosome arm that harbored the bulk of these genes, 7/30 DEGs were located on the primarily heterochromatic 4th chromosome. Interestingly, 21 of the remaining 23 DEGs were located in centromere-proximal locations along their respective chromosome arms. A metaplot of these 23 genes from State 7 is shown in Fig. 5d, showing that all but one of them were derepressed in the mutant. Note that the genome build for these regions is incomplete, and so, the relative position of the centromere is not the same for each arm. Thus, the metaplot is not meant to depict the precise location of each DEG but rather to illustrate its general positioning along the arm. Nevertheless, the results collectively provide strong evidence that loss of H3.3 K36 results in derepression of genes located in heterochromatic regions of the genome.

H3.3^{K36R} mutants exhibit position effects in the adult eye

In contrast with its typical role as a marker of active genes along chromosome arms, H3.3 is also known to be deposited by the ATRX•Daxx complex to maintain repressive pericentric and (sub)telomeric chromatin (Wong *et al.* 2009; Drane *et al.* 2010; Lewis *et al.* 2010). In mouse embryonic stem cells, loss of H3f3a and H3f3b (orthologs of H3.3A and H3.3B in flies) results in reduced levels of H3K9me3 and ATRX at telomeres (Udugama *et al.* 2015). The chromatin state analysis of H3.3^{K36R} DEGs shown in Fig. 5 clearly implicates a disruption to H3K9-mediated silencing, particularly in centromere-proximal regions. However, due to the paucity of protein coding genes located near telomeres, this approach is unable to evaluate the transcriptional status of telomere-proximal heterochromatin.

The fruitfly genome is rare among eukaryotes because it does not encode a telomerase RNP (Mason *et al.* 2008). Instead, telomere length is maintained by controlled retrotransposition of HeT-A (Healing Transposon A), TART (Telomere Associated Retrotransposon), and TAHRE (Telomere Associated and HeT-A Related) elements into a telomere-proximal region (Fig. 6a). Telomeric chromatin is comprised of two distinct epigenetic compartments that are believed to perform different functions. The so-called HTT (HeT-A, TART, TAHRE) array (Fig. 6a), is primarily marked by H3K9 methylation that is thought to be required for proper expression of the HTT array (Mason *et al.* 2008; Cacchione *et al.* 2020). Adjacent to the array are the Telomere Associated Sequences (TAS, Fig. 6a), which contain 40–60 copies of telomere-specific satellite repeats per chromosome arm (Mason *et al.* 2008; Antao *et al.* 2012). Interestingly, TAS repeats are marked by repressive H3K27me3 and Polycomb Group (PcG) proteins (Boivin *et al.* 2003).

In order to assay the functional consequences of H3.3^{K36R} mutation at telomeres, we utilized a miniwhite reporter system pioneered by Wallrath and Elgin (Wallrath and Elgin 1995). These and other reporters have been widely used to analyze PEV of the *white* gene in the adult *Drosophila* eye (Fig. 6a). We ingressed six different *hsp70-w* reporter transgenes, located either on 3R or YS, into the background of H3.3A^{null} or H3.3^{K36R} mutants. Five of these lines contain insertions in telomeric chromatin (two in TAS on 3R; two in the HTT array of the Y chromosome), and one of them (118-E12) is inserted near centric heterochromatin on 3R

(Fig. 6b). Surprisingly, none of the HTT reporters on the Y chromosome showed appreciable differences in the intensity or extent of PEV in the K36R mutant eyes, compared to the controls (Fig. 6b). In contrast, each of the TAS reporters on 3R showed an increase in the overall intensity of red eye pigmentation compared to the basal levels of the control animals. Also note that Y chromosome reporters showed significant variegation, whereas the 3R lines had more uniform expression levels. Although the basal level of pigmentation in 118-E6 is quite high, and that of line 118-E12 is rather low, we consistently found slightly higher levels in the K36R animals (Fig. 6b and Supplementary Fig. 6). This effect is more clearly seen in line 39C-62, which has moderate basal levels and demonstrably higher levels in the presence of the K36R mutation (Fig. 6b). These observations indicate that H3.3K36 may play a role in maintaining a suppressive chromatin environment within TAS as well as centric heterochromatin.

Loss of H3.3 K36 reduces expression of telomere-specific retroposons but causes derepression of many other TEs

The role of ATRX•Daxx-mediated H3.3 deposition in promoting and maintaining the silencing of TEs is a well-documented feature of higher eukaryotic genomes (Elsässer *et al.* 2015; Sadic *et al.* 2015; Groh *et al.* 2021). Thus, we were curious to directly determine whether transcription of telomeric transposons was altered. Because transposons are repetitive elements, traditional RNA-seq pipelines are not set up to properly apportion short sequencing reads to repeat-rich regions of the genome. Hence, differential analysis of transposable element (TE) expression was performed using the open source software package, TEsTranscripts (Jin *et al.* 2015). A volcano plot of these data is shown in Fig. 6c, revealing a dramatic TE derepression phenotype. Prominent among the classes of upregulated TEs are LTR-type retrotransposons (Fig. 6, c and d). Increasing mobilization of transposons leading to DNA damage has also been associated with aging (Cardelli 2018; Ochoa Thomas *et al.* 2020). These data suggest that activation of repressed TEs may contribute to the reduced lifespan of H3.3^{K36R} mutant animals.

Conspicuous among the TE families that are downregulated in K36R mutants is the HeT-A family of LINE-like (non-LTR) retroposons involved in telomere length maintenance. As shown in Fig. 6c, expression of transcripts corresponding to the HeT-A family is dramatically reduced in old K36R mutant vs control fly heads. Note that we also found that expression of both HeT-A and TART elements was significantly reduced in the old K36R mutants if we employed the more commonly-used featureCounts tool instead of TEcounts (see Supplementary Tables 2 and 3). Among the three telomeric retrotransposons, HeT-A elements are particularly important because the HeT-A Orf1p/Gag protein recruits its TART counterpart to chromosome ends (Pardue *et al.* 2005; Casacuberta 2017). Thus, reduced expression of HeT-A elements would be expected to have serious consequences for telomeric stability (Silva-Sousa *et al.* 2012). Telomere shortening is a well-known hallmark of cellular senescence; these data are consistent with the notion that defects in telomere maintenance contribute to the observed reduced lifespan phenotype in H3.3^{K36R} animals.

Hyperacetylation of histone H4 in H3.3K36R chromatin

Our finding of impaired heterochromatic silencing in H3.3K36R mutants aligns well with previous observations of senescence-associated heterochromatin defects in aging insects (Wood *et al.* 2010, 2016) as well as in senescent mammalian cells (Sen *et al.* 2015; Dasgupta *et al.* 2023). Another hallmark of senescent cells

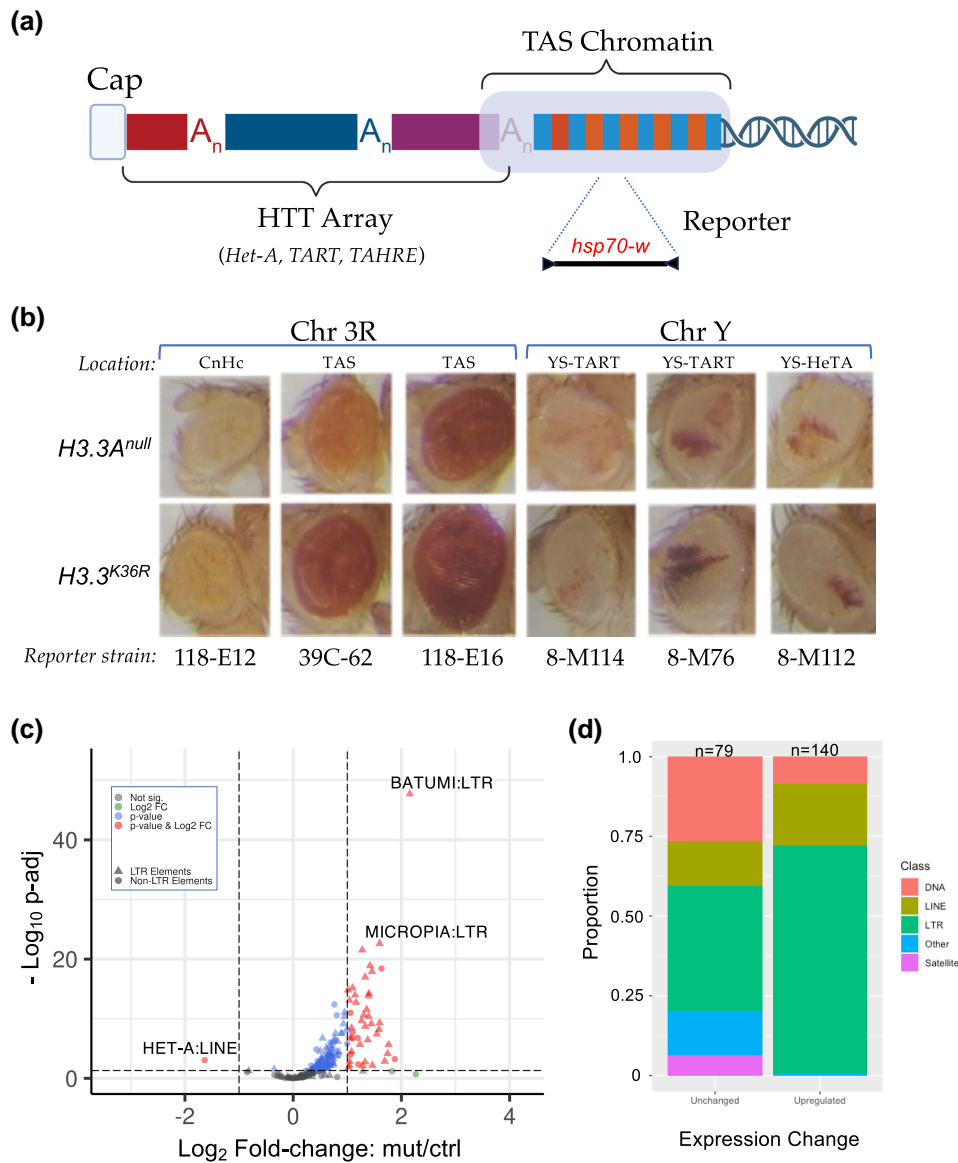


Fig. 6. Telomeric position effect and TE expression analysis. a) Cartoon depicting key features of *Drosophila* telomeres. At the distal end of the telomere, a capping complex assembles adjacent to arrays of *Het-A*, *TAHRE*, and *TART* retrotransposons (HTT array). Proximal to that is the TAS (Telomere Associated Sequence) Chromatin, which is characterized by the presence of complex satellite repeats that vary by chromosome. b) Images of adult eyes. For each column, representative examples are shown for a particular reporter strain. Rows correspond to genotype (*H3.3A^{null}* control or *H3.3^{K36R}* mutant). The location and type of chromatin for each reporter strain is also indicated: Pericentric heterochromatin (CnHc), TAS, YS-TART (Y chromosome TART), and YS-HeTA (Y chromosome HeT-A). *n*-values for each experiment ranged from 16 to 44, see [Supplementary Fig. 6](#) for details. c) Volcano plot of annotated TEs analyzed using the TEcounts tool within TETRascripts. Each dot or triangle represents the combined reads from all loci for a given TE subtype. Dotted lines represent significance cutoffs for adjusted *P*-value and \log_2 -fold change. Symbols are color coded according to the key in the upper left. LTR-type transposons are represented by triangles, non-LTR elements are shown as dots. d) Stacked bar graph, binned by whether TEs were upregulated or unchanged in the *H3.3^{K36R}* mutant. The relative proportion of a given type of TE (DNA, LINE, LTR, Satellite, and Other) in each bin are shaded as indicated in the legend.

and tissues are changes in the acetylation status of histone H4 [reviewed in [Graff and Tsai \(2013\)](#), [Benayoun et al. \(2015\)](#), and [Peleg et al. \(2016b\)](#)]. Indeed, these changes in histone acetylation patterns are often already apparent when animals reach midlife ([Peleg et al. 2016a](#)). Using a multi-gene replacement strategy to analyze functions of the replication-dependent H3.2 histones ([McKay et al. 2015](#); [Meers et al. 2018](#)), we previously showed that an *H3.2K36R* mutation caused global hyperacetylation of H4 ([Meers et al. 2017](#)). To determine if an *H3.3K36R* substitution might have a similar effect, we measured overall histone H4 acetylation levels in mutant and control animals by western blotting.

As shown in [Fig. 7](#), we assayed bulk levels of histone H4ac and H3 (loading control) and found that acetylated H4 was significantly higher in *H3.3K36R* mutants compared to *H3.3A^{null}* or *yw* control animals. Confirming the previously identified link between *H3K36me* and H4ac in yeast, these findings are also consistent with the idea that Set2-mediated K36 trimethylation recruits the histone deacetylase complex, RPD3S ([Carrozza et al. 2005](#); [Keogh et al. 2005](#)). Histone hyperacetylation has long been regarded as a dynamic characteristic of transcriptionally active genes, a property associated with elongating polymerases ([Cho et al. 1998](#)).

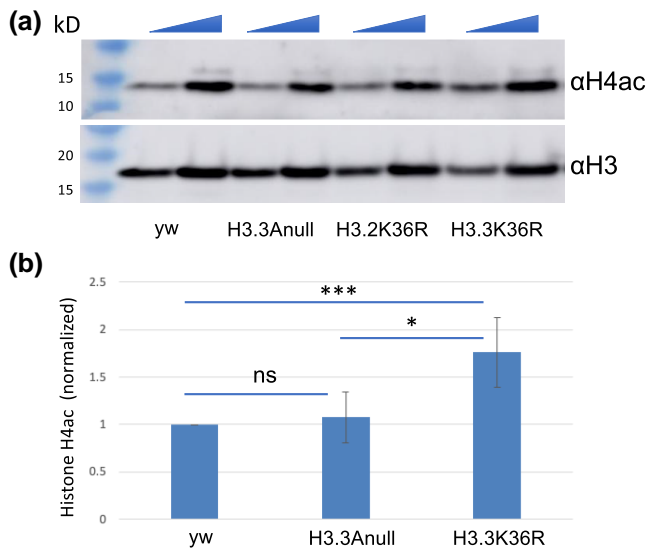


Fig. 7. Hyperacetylation of histone H4 in H3.3K36R mutants. Western blotting for pan H4 acetylation (H4ac) and anti-H3 on lysates from WL3 larvae. a) Representative gel image. yw and H3.3Anull controls are shown along with H3.3K36R mutants. The H3.2K36R lanes are provided for visual comparison but are not quantified (see Methods for details). As indicated by the triangles at the top edge for each pair of lanes per genotype, either 20 or 40 μ g of total protein per lane was loaded. b) Quantification of the data from three independent replicates. Mean pixel intensity for each band was measured, and ratio of H4ac/H3 was computed per replicate. For each experiment, the H4ac/H3 ratio of mutant genotypes was normalized to the H3.3A^{null} control. For each genotype, normalized means and SD were plotted. Significance between raw H4ac/H3 ratios was assessed by paired one-way ANOVA, followed by Friedman tests comparing mutant genotypes to H3.3A^{null} controls. P values are indicated as follows: *** < 0.001; * < 0.05; ns = not significant.

Recently, an investigation of diverse metazoan species, including *Drosophila*, found that transcription elongation rates naturally increase with organismal age, and that reducing Pol II speed extends lifespan (Debes et al. 2023). Given that histone H4 acetylation is known to destabilize nucleosomes during transcription [reviewed in Henikoff (2008)], activities that serve to hyperacetylate histones would be expected to increase polymerase elongation rates. Taken together, our findings are consistent with the notion that hyperacetylation of H4 may contribute to the premature lethality of H3.3K36R mutant flies.

Discussion

Aging is a complex process that involves multiple factors contributing to the decline of cellular and organismal functions, ultimately leading to decreased lifespan. Cellular senescence is characterized by numerous features, including irreversible cell cycle arrest, altered gene expression patterns, metabolic changes, and the acquisition of a SASP. Senescent cells secrete pro-inflammatory cytokines, growth factors, and matrix remodeling enzymes, contributing to chronic inflammation, tissue dysfunction, and age-related pathologies. Epigenetic changes, including histone modifications, have been identified as crucial contributors to aging-related processes. In this study, we focused on the lysine-36 residue of the replication-independent histone protein, H3.3. Our results demonstrate that expression of H3.3K36R as the sole source of H3.3 protein causes a significant reduction in adult lifespan and dysregulation of the genomic and transcriptomic architecture. Genetic rescue of the longevity defect upon transgenic co-expression of wild-type H3.3B

suggests an important role for lysine-36 in supporting longevity. Additionally, our transcriptome profiling of young and aged adult fly heads reveals age-dependent misexpression of innate immune target genes, hyperacetylation of histone H4, and derepression of heterochromatic transcripts in H3.3K36R mutants.

Role of Toll/Imd pathways in aging and immunosenescence

The Toll/Imd pathways are thought to play a vital role in regulating immunity and are intertwined with the aging process. Knockdown of Toll/Imd pathway members extends lifespan, whereas their overexpression shortens it (Khor and Cai 2020). Immunosenescence, characterized by age-dependent decline in immune function, is a hallmark of the aging process (DeVeale et al. 2004; Muller et al. 2013). Interestingly, both sexes become more susceptible to infection as they age, with different underlying mechanisms. For males, susceptibility is primarily posited to be caused by deterioration in barrier defenses, whereas for females, systemic immune defense senescence is thought to be the major contributor (Kubiak and Tinsley 2017).

Our findings are also consistent with observations in mammals, wherein NF- κ B activity increases over time in the brains of middle-aged and older mice relative to young mice (Zhang et al. 2013). The upregulation of AMP expression in aged *Drosophila* (Kounatidis et al. 2017) further supports the connection between immune signaling and the aging process. Notably, downregulation of NF- κ B has been shown to mobilize nutrients and extend lifespan, whereas its overexpression has been linked to neurodegeneration (Zhang et al. 2013; Kounatidis et al. 2017). Our investigation into the molecular consequences of the H3.3^{K36R} substitution highlights its involvement in regulating critical aspects of immune signaling and heterochromatic silencing. Using a statistical interaction model, we discerned the effects of age and sex on gene expression in H3.3^{K36R} mutants compared to controls. Notably, the expression of downstream targets of NF- κ B signaling, such as AMPs and other immune effectors, were upregulated in the mutants. This suggests that H3.3K36 may play a role in suppressing immune responses in the absence of external immune challenge, thereby contributing to the maintenance of cellular homeostasis in the adult brain.

H3.3K36, retrotransposition and Senescence

Understanding the intricate interplay between chromatin dynamics and the aging process should offer valuable insights into mechanisms of aging and age-related diseases. Upon loss of H3.3K36, our analysis has revealed a disruption of H3K9-mediated silencing in both centromere- and telomere-proximal regions. This includes a robust downregulation of non-LTR retrotransposons that are critical for maintaining telomere length (Pardue et al. 2005; Casacuberta 2017). In contrast, the observed derepression of genes and LTR-type retrotransposons in heterochromatic regions provides strong evidence that H3.3K36 is involved in maintaining repressive pericentric and subtelomeric chromatin, possibly through ATRX•Daxx-mediated deposition. Consistent with these observations, Groth and colleagues have shown that DAXX provides additional functionality to the histone chaperone system by recruiting H3K9 methyltransferases (Carraro et al. 2023). The same group recently showed that a failure to re-establish H3K9me in postreplicative mammalian chromatin causes derepression of LTR-type retrotransposons (Wenger et al. 2023). While this work was under revision, another group found that expression of a “domesticated” capsid gene derived from an LTR-retrotransposon supports adult longevity in *Drosophila* (Balakireva et al. 2024). Taken together with our work, these findings

strongly suggest that H3.3K36 plays a conserved and specific role in silencing these so-called genomic parasites.

We also observed that mutation of H3.3K36 results in increased expression of reporters in H3K27me3 marked TAS and reduced expression of chromatin State 6 genes (marked by H3K27me3 and Pc proteins). These findings are in line with our recent work suggesting a role for H3.3K36 in maintaining the function of genes marked by H3K27me3 (Salzler et al. 2023). Studies in many organisms point to gene regulation by PcG proteins as another pathway that influences longevity (Siebold et al. 2010; Ni et al. 2012; Sen et al. 2016; Ma et al. 2018). However, the evidence is inconsistent between organisms, and much remains to be learned mechanistically. Further work clarifying the relationship between H3.3K36, Polycomb mediated gene repression, and aging would be an interesting area of future investigation.

It is intriguing to speculate on mechanisms through which H3.3K36 might support retrotransposon expression at telomeres. One possibility is that this residue facilitates expression of piRNA pathway genes. The piRNA pathway functions to suppress transposon activity in the germline, including activity of the HTT array (Savitsky et al. 2006; Brennecke et al. 2007; Klattenhoff et al. 2009; Mohn et al. 2014). Consistent with our observation of downregulation of HeT-A and widespread derepression of other TE families in H3.3^{K36R} mutants, previous studies have observed differences in regulation of telomeric piRNA clusters compared to those that target nontelomeric TEs (Klattenhoff et al. 2009; Mohn et al. 2014). Furthermore, analysis of a dominant negative H3.3^{K36M} model (causing reduction in methylation of both H3.2K36 and H3.3K36), showed that telomeric retrotransposons were downregulated by piRNA pathway genes (Chaouch et al. 2021). In H3.3^{K36M} mutant eye-antennal discs, suppression of HeT-A levels was elicited by upregulation of the piRNA promoting gene, *krimp*. Importantly, the suppression of HeT-A levels in these mutants could be rescued solely by reducing *krimp* expression (Chaouch et al. 2021). Of note, we also observe upregulation of *krimp* in old H3.3^{K36R} mutants (log₂-fold change = ~1.3), as well as another piRNA pathway gene, *Ago3* (log₂-fold change = ~1.2), see Supplementary Table 1 for details.

Another mechanism through which H3.3K36 might sustain expression of the HTT array is by promoting Jil-1 kinase function. Phosphorylation of the Jil-1 target, histone H3 serine 10, antagonizes both methylation of H3K9 and gene repression (Zhang et al. 2006; Bao et al. 2007). Jil-1 is a positive regulator of HTT transcript levels (Silva-Sousa et al. 2012; Silva-Sousa and Casacuberta 2013). Moreover, *Jil-1* and H3.3^{K36R} mutants both exhibit repression of HeT-A transcription and suppression of TAS-reporter transgenes (Silva-Sousa et al. 2012; this work). Recently, an H3K36me3 reader protein, Jasper, has emerged as an important factor for stabilization and recruitment of Jil-1 (Albig et al. 2019; Dou et al. 2020). *Jasper* mutants exhibit both an increase in H3K9me2 and a decrease in expression of HeT-A and TART transposons (Albig et al. 2019). However, unlike H3.3^{K36R} mutants, *Jil-1* and *Jasper* mutants do not exhibit widespread derepression of transposons in other parts of the genome (Albig et al. 2019; Dou et al. 2020). An interesting area of future study would be to determine whether this difference might be due to activities specific to H3.2K36 vs H3.3K36.

In summary, we find that lysine-36 of *Drosophila* histone H3.3 is crucial for supporting adult longevity by regulating immune signaling, heterochromatic silencing, and retrotransposon repression. The dysregulation of these processes in H3.3K36R mutants likely contributes to age-related changes in gene expression and chromatin organization, ultimately impacting organismal lifespan. Further investigations into the mechanistic details of how H3.3K36 functions in these pathways will shed light on the broader role of histone

modifications in the aging process. Additionally, exploring the conservation of these mechanisms in other organisms, including mammals, may have implications for understanding aging and age-related diseases in humans. Future studies of this process in model organisms may also provide potential therapeutic targets to mitigate age-related decline and improve healthy aging.

Data availability statement

Fly strains are available upon request. Gene expression data are available at GEO with the accession number: GSE244389. Code and workflows used for data processing and gene expression analysis can be found at <https://doi.org/10.5281/zenodo.10553305>. Supplemental files include: Supplementary Figs. 1-6 and Supplementary Tables 1-3. Supplementary Table 1: file of all 483 DEGs identified in the interaction model, together with relevant statistics (P-value, LFC etc.). Supplementary Table 2: file of all differentially expressed transposon elements (TE DEGs) using the TEcounts tool. Supplementary Table 3: file of all differentially expressed transposon elements (TE DEGs) using the featureCounts tool.

Supplemental material available at G3 online.

Acknowledgments

The authors thank D. McKay, R. Duronio and J-M. McPherson for advice and critical reading of the manuscript.

Funding

This work was supported by National Institutes of Health grant R35-GM136435 (to A.G.M.).

Conflicts of interest

The author(s) declare no conflict of interest.

Literature cited

- Akhmanova AS, Bindels PC, Xu J, Miedema K, Kremer H, Hennig W, Xu J, Hennig W. 1995. Structure and expression of histone H3.3 genes in *Drosophila melanogaster* and *Drosophila hydei*. *Genome*. 38(3):586–600. doi:10.1139/g95-075.
- Albig C, Wang C, Dann GP, Wojcik F, Schauer T, Krause S, Maenner S, Cai W, Li Y, Girton J, et al. 2019. JASPer controls interphase histone H3S10 phosphorylation by chromosomal kinase JIL-1 in *Drosophila*. *Nat Commun*. 10(1):5343. doi:10.1038/s41467-019-13174-6.
- Andrews S. 2010. FastQC: a Quality Control Tool for High Throughput Sequence Data, pp. Babraham Bioinformatics, Babraham Institute. United Kingdom: Cambridge.
- Antao JM, Mason JM, Dejardin J, Kingston RE. 2012. Protein landscape at *Drosophila melanogaster* telomere-associated sequence repeats. *Mol Cell Biol*. 32(12):2170–2182. doi:10.1128/MCB.00010-12.
- Aron L, Zullo J, Yankner BA. 2022. The adaptive aging brain. *Curr Opin Neurobiol*. 72:91–100. doi:10.1016/j.conb.2021.09.009.
- Ashburner M, Ball CA, Blake JA, Botstein D, Butler H, Cherry JM, Davis AP, Dolinski K, Dwight SS, Eppig JT, et al. 2000. Gene ontology: tool for the unification of biology. The gene ontology consortium. *Nat Genet*. 25(1):25–29. doi:10.1038/75556.
- Balakireva Y, Nikitina M, Makhnovskii P, Kukushkina I, Kuzmin I, Kuzmin I, Kim A, Nefedova L. 2024. The lifespan of *D. melanogaster* depends on the function of the *Gagr* gene, a domesticated *gag*

- gene of *Drosophila* LTR retrotransposons. *Insects*. 15(1):68. doi:10.3390/insects15010068.
- Bannister AJ, Kouzarides T. 2011. Regulation of chromatin by histone modifications. *Cell Res*. 21(3):381–395. doi:10.1038/cr.2011.22.
- Bao X, Deng H, Johansen J, Girton J, Johansen KM. 2007. Loss-of-function alleles of the JIL-1 histone H3S10 kinase enhance position-effect variegation at pericentric sites in *Drosophila* heterochromatin. *Genetics*. 176(2):1355–1358. doi:10.1534/genetics.107.073676.
- Bell O, Tiwari VK, Thoma NH, Schubeler D. 2011. Determinants and dynamics of genome accessibility. *Nat Rev Genet*. 12(8):554–564. doi:10.1038/nrg3017.
- Benayoun BA, Pollina EA, Brunet A. 2015. Epigenetic regulation of ageing: linking environmental inputs to genomic stability. *Nat Rev Mol Cell Biol*. 16(10):593–610. doi:10.1038/nrm4048.
- Boivin A, Gally C, Netter S, Anxolabehere D, Ronssey S. 2003. Telomeric associated sequences of *Drosophila* recruit polycomb-group proteins in vivo and can induce pairing-sensitive repression. *Genetics*. 164(1):195–208. doi:10.1093/genetics/164.1.195.
- Brennecke J, Aravin AA, Stark A, Dus M, Kellis M, Sachidanandam R, Hannon GJ. 2007. Discrete small RNA-generating loci as master regulators of transposon activity in *Drosophila*. *Cell*. 128(6):1089–1103. doi:10.1016/j.cell.2007.01.043.
- Cacchione S, Cenci G, Raffa GD. 2020. Silence at the End: how *Drosophila* regulates expression and transposition of telomeric retroelements. *J Mol Biol*. 432(15):4305–4321. doi:10.1016/j.jmb.2020.06.004.
- Cardelli M. 2018. The epigenetic alterations of endogenous retroelements in aging. *Mech Ageing Dev*. 174:30–46. doi:10.1016/j.mad.2018.02.002.
- Carraro M, Hendriks IA, Hammond CM, Solis-Mezarino V, Volker-Albert M, Elsborg JD, Weisser MB, Spanos C, Montoya G, Rappsilber J, et al. 2023. DAXX adds a de novo H3.3K9me3 deposition pathway to the histone chaperone network. *Mol Cell*. 83(7):1075–1092 e1079. doi:10.1016/j.molcel.2023.02.009.
- Carrozza MJ, Li B, Florens L, Suganuma T, Swanson SK, Lee KK, Shia W-J, Anderson S, Yates J, Washburn MP, et al. 2005. Histone H3 methylation by Set2 directs deacetylation of coding regions by Rpd3S to suppress spurious intragenic transcription. *Cell*. 123(4):581–592. doi:10.1016/j.cell.2005.10.023.
- Casacuberta E. 2017. *Drosophila*: retrotransposons making up telomeres. *Viruses*. 9(7):192. doi:10.3390/v9070192.
- Chaouch A, Berlandi J, Chen CCL, Frey F, Badini S, Harutyunyan AS, Chen X, Krug B, Hébert S, Jeibmann A, et al. 2021. Histone H3.3 K27M and K36M mutations de-repress transposable elements through perturbation of antagonistic chromatin marks. *Mol Cell*. 81(23):4876–4890.e7. doi:10.1016/j.molcel.2021.10.008.
- Childs BG, Durik M, Baker DJ, van Deursen JM. 2015. Cellular senescence in aging and age-related disease: from mechanisms to therapy. *Nat Med*. 21(12):1424–1435. doi:10.1038/nm.4000.
- Cho H, Orphanides G, Sun X, Yang XJ, Ogryzko V, Lees E, Nakatani Y, Reinberg D. 1998. A human RNA polymerase II complex containing factors that modify chromatin structure. *Mol Cell Biol*. 18(9):5355–5363. doi:10.1128/MCB.18.9.5355.
- Clapier CR, Iwasa J, Cairns BR, Peterson CL. 2017. Mechanisms of action and regulation of ATP-dependent chromatin-remodelling complexes. *Nat Rev Mol Cell Biol*. 18(7):407–422. doi:10.1038/nrm.2017.26.
- Dasgupta N, Lei X, Arnold R, Teneche MG, Miller KN, Rajesh A, Davis A, Anschau V, Campos AR, Gilson R, et al. 2023. Histone chaperone HIRA, Promyelocytic Leukemia (PML) protein and p62/SQSTM1 coordinate to regulate inflammation during cell senescence and aging. *bioRxiv*: 2023.2006.2024.546372.
- Debes C, Papadakis A, Gronke S, Karalay O, Tain LS, Mizi A, Nakamura S, Hahn O, Weigelt C, Josipovic N, et al. 2023. Ageing-associated changes in transcriptional elongation influence longevity. *Nature*. 616(7958):814–821. doi:10.1038/s41586-023-05922-y.
- DeVeale B, Brummel T, Seroude L. 2004. Immunity and aging: the enemy within? *Aging Cell*. 3(4):195–208. doi:10.1111/j.1474-9728.2004.00106.x.
- Dobin A, Davis CA, Schlesinger F, Drenkow J, Zaleski C, Jha S, Batut P, Chaisson M, Gingeras TR. 2013. STAR: ultrafast universal RNA-seq aligner. *Bioinformatics*. 29(1):15–21. doi:10.1093/bioinformatics/bts635.
- Dou K, Liu Y, Zhang Y, Wang C, Huang Y, Zhang ZZ. 2020. *Drosophila* p75 safeguards oogenesis by preventing H3K9me2 spreading. *J Genet Genomics*. 47(4):187–199. doi:10.1016/j.jgg.2020.02.008.
- Drane P, Ouararhni K, Depaux A, Shuaib M, Hamiche A. 2010. The death-associated protein DAXX is a novel histone chaperone involved in the replication-independent deposition of H3.3. *Genes Dev*. 24(12):1253–1265. doi:10.1101/gad.566910.
- Eberharther A, Becker PB. 2002. Histone acetylation: a switch between repressive and permissive chromatin. Second in review series on chromatin dynamics. *EMBO Rep*. 3(3):224–229. doi:10.1093/embo-reports/kvf053.
- Elsässer SJ, Goldberg AD, Allis CD. 2010. New functions for an old variant: no substitute for histone H3.3. *Curr Opin Genet Dev*. 20(2):110–117. doi:10.1016/j.gde.2010.01.003.
- Elsässer SJ, Noh KM, Diaz N, Allis CD, Banaszynski LA. 2015. Histone H3.3 is required for endogenous retroviral element silencing in embryonic stem cells. *Nature*. 522(7555):240–244. doi:10.1038/nature14345.
- Filipescu D, Szenker E, Almouzni G. 2013. Developmental roles of histone H3 variants and their chaperones. *Trends Genet*. 29(11):630–640. doi:10.1016/j.tig.2013.06.002.
- Garschall K, Flatt T. 2018. The interplay between immunity and aging in *Drosophila*. *F1000Res*. 7:160. doi:10.12688/f1000research.13117.1.
- Gene Ontology Consortium, Aleksander SA, Balhoff J, Carbon S, Cherry JM, Drabkin HJ, Ebert D, Feuermann M, Gaudet P, Harris NL, et al. 2023. The gene ontology knowledgebase in 2023. *Genetics*. 224(1):iyad031. doi:10.1093/genetics/iyad031.
- Graff J, Tsai LH. 2013. Histone acetylation: molecular mnemonics on the chromatin. *Nat Rev Neurosci*. 14(2):97–111. doi:10.1038/nrn3427.
- Gramates LS, Agapite J, Attrill H, Calvi BR, Crosby MA, dos Santos G, Goodman JL, Goutte-Gattat D, Jenkins VK, Kaufman T, et al. 2022. FlyBase: a guided tour of highlighted features. *Genetics*. 220(4):iyac035. doi:10.1093/genetics/iyac035.
- Groh S, Milton AV, Marinelli LK, Sickingner CV, Russo A, Bollig H, de Almeida GP, Schmidt A, Forné I, Imhof A, et al. 2021. Morc3 silences endogenous retroviruses by enabling daxx-mediated histone H3.3 incorporation. *Nat Commun*. 12(1):5996. doi:10.1038/s41467-021-26288-7.
- Gusarov I, Shamovsky I, Pani B, Gautier L, Eremina S, Katkova-Zhukotskaya O, Mironov A, Makarov AA, Nudler E. 2021. Dietary thiols accelerate aging of *C. elegans*. *Nat Commun*. 12(1):4336. doi:10.1038/s41467-021-24634-3.
- Hanson MA, Cohen LB, Marra A, Iatsenko I, Wasserman SA, Lemaitre B. 2021. The *Drosophila* Baramicin polypeptide gene protects against fungal infection. *PLoS Pathog*. 17(8):e1009846. doi:10.1371/journal.ppat.1009846.
- Henikoff S. 2008. Nucleosome destabilization in the epigenetic regulation of gene expression. *Nat Rev Genet*. 9(1):15–26. doi:10.1038/nrg2206.
- Iskusnykh IY, Zakharova AA, Pathak D. 2022. Glutathione in brain disorders and aging. *Molecules*. 27(1):324. doi:10.3390/molecules27010324.
- Ji S, Luo Y, Cai Q, Cao Z, Zhao Y, Mei J, Li C, Xia P, Xie Z, Xia Z, et al. 2019. LC Domain-Mediated coalescence is essential for otu

- enzymatic activity to extend *Drosophila* lifespan. *Mol Cell*. 74(2): 363–377.e5. doi:[10.1016/j.molcel.2019.02.004](https://doi.org/10.1016/j.molcel.2019.02.004).
- Jin Y, Tam OH, Paniagua E, Hammell M. 2015. TEtranscripts: a package for including transposable elements in differential expression analysis of RNA-seq datasets. *Bioinformatics*. 31(22): 3593–3599. doi:[10.1093/bioinformatics/btv422](https://doi.org/10.1093/bioinformatics/btv422).
- Keogh MC, Kurdistani SK, Morris SA, Ahn SH, Podolny V, Collins SR, Schuldiner M, Chin K, Punna T, Thompson NJ, et al. 2005. Cotranscriptional set2 methylation of histone H3 lysine 36 recruits a repressive Rpd3 complex. *Cell*. 123(4):593–605. doi:[10.1016/j.cell.2005.10.025](https://doi.org/10.1016/j.cell.2005.10.025).
- Kharchenko PV, Alekseyenko AA, Schwartz YB, Minoda A, Riddle NC, Ernst J, Sabo PJ, Larschan E, Gorchakov AA, Gu T, et al. 2011. Comprehensive analysis of the chromatin landscape in *Drosophila melanogaster*. *Nature*. 471(7339):480–485. doi:[10.1038/nature09725](https://doi.org/10.1038/nature09725).
- Khor S, Cai D. 2020. Control of lifespan and survival by *Drosophila* NF-kappaB signaling through neuroendocrine cells and neuroblasts. *Aging (Albany NY)*. 12(24):24604–24622. doi:[10.18632/aging.104196](https://doi.org/10.18632/aging.104196).
- Klattenhoff C, Xi H, Li C, Lee S, Xu J, Khurana JS, Zhang F, Schultz N, Koppetsch BS, Nowosielska A, et al. 2009. The *Drosophila* HP1 homolog Rhino is required for transposon silencing and piRNA production by dual-strand clusters. *Cell*. 138(6):1137–1149. doi:[10.1016/j.cell.2009.07.014](https://doi.org/10.1016/j.cell.2009.07.014).
- Konev AY, Tribus M, Park SY, Podhraski V, Lim CY, Emelyanov AV, Vershilova E, Pirrotta V, Kadonaga JT, Lusser A, et al. 2007. CHD1 motor protein is required for deposition of histone variant H3.3 into chromatin in vivo. *Science*. 317(5841):1087–1090. doi:[10.1126/science.1145339](https://doi.org/10.1126/science.1145339).
- Kounatidis I, Chtarbanova S, Cao Y, Hayne M, Jayanth D, Ganetzky B, Ligoxygakis P. 2017. NF-kappaB Immunity in the brain determines fly lifespan in healthy aging and age-related neurodegeneration. *Cell Rep*. 19(4):836–848. doi:[10.1016/j.celrep.2017.04.007](https://doi.org/10.1016/j.celrep.2017.04.007).
- Kubiak M, Tinsley MC. 2017. Sex-specific routes to immune senescence in *Drosophila melanogaster*. *Sci Rep*. 7(1):10417. doi:[10.1038/s41598-017-11021-6](https://doi.org/10.1038/s41598-017-11021-6).
- Lewis PW, Elsaesser SJ, Noh KM, Stadler SC, Allis CD. 2010. Daxx is an H3.3-specific histone chaperone and cooperates with ATRX in replication-independent chromatin assembly at telomeres. *Proc Natl Acad Sci U S A*. 107(32):14075–14080. doi:[10.1073/pnas.1008850107](https://doi.org/10.1073/pnas.1008850107).
- Li B, Carey M, Workman JL. 2007. The role of chromatin during transcription. *Cell*. 128(4):707–719. doi:[10.1016/j.cell.2007.01.015](https://doi.org/10.1016/j.cell.2007.01.015).
- Liao Y, Smyth GK, Shi W. 2014. featureCounts: an efficient general purpose program for assigning sequence reads to genomic features. *Bioinformatics*. 30(7):923–930. doi:[10.1093/bioinformatics/btt656](https://doi.org/10.1093/bioinformatics/btt656).
- Lindsay SA, Lin SJH, Wasserman SA. 2018. Short-form bomanins mediate humoral immunity in *Drosophila*. *J Innate Immun*. 10(4): 306–314. doi:[10.1159/000489831](https://doi.org/10.1159/000489831).
- Liu H, Wang H, Shenvi S, Hagen TM, Liu RM. 2004. Glutathione metabolism during aging and in Alzheimer disease. *Ann N Y Acad Sci*. 1019(1):346–349. doi:[10.1196/annals.1297.059](https://doi.org/10.1196/annals.1297.059).
- Lorch Y, LaPointe JW, Kornberg RD. 1987. Nucleosomes inhibit the initiation of transcription but allow chain elongation with the displacement of histones. *Cell*. 49(2):203–210. doi:[10.1016/0092-8674\(87\)90561-7](https://doi.org/10.1016/0092-8674(87)90561-7).
- Love MI, Huber W, Anders S. 2014. Moderated estimation of fold change and dispersion for RNA-seq data with DESeq2. *Genome Biol*. 15(12):550. doi:[10.1186/s13059-014-0550-8](https://doi.org/10.1186/s13059-014-0550-8).
- Ma Z, Wang H, Cai Y, Wang H, Niu K, Wu X, Ma H, Yang Y, Tong W, Liu F, et al. 2018. Epigenetic drift of H3K27me3 in aging links glycolysis to healthy longevity in *Drosophila*. *Elife*. 7:e35368. doi:[10.7554/eLife.35368](https://doi.org/10.7554/eLife.35368).
- Mason JM, Frydrychova RC, Biessmann H. 2008. *Drosophila* telomeres: an exception providing new insights. *Bioessays*. 30(1): 25–37. doi:[10.1002/bies.20688](https://doi.org/10.1002/bies.20688).
- Mavrogonatou E, Papadopoulou A, Pratsinis H, Kletsas D. 2023. Senescence-associated alterations in the extracellular matrix: deciphering their role in the regulation of cellular function. *Am J Physiol Cell Physiol*. 325(3):C633–C647. doi:[10.1152/ajpcell.00178.2023](https://doi.org/10.1152/ajpcell.00178.2023).
- McKay DJ, Klusza S, Penke TJ, Meers MP, Curry KP, McDaniel SL, Malek PY, Cooper SW, Tatomer DC, Lieb JD, et al. 2015. Interrogating the function of metazoan histones using engineered gene clusters. *Dev Cell*. 32(3):373–386. doi:[10.1016/j.devcel.2014.12.025](https://doi.org/10.1016/j.devcel.2014.12.025).
- McKitttrick E, Gafken PR, Ahmad K, Henikoff S. 2004. Histone H3.3 is enriched in covalent modifications associated with active chromatin. *Proc Natl Acad Sci U S A*. 101(6):1525–1530. doi:[10.1073/pnas.0308092100](https://doi.org/10.1073/pnas.0308092100).
- Mebratu YA, Soni S, Rosas L, Rojas M, Horowitz JC, Nho R. 2023. The aged extracellular matrix and the profibrotic role of senescence-associated secretory phenotype. *Am J Physiol Cell Physiol*. 325(3): C565–C579. doi:[10.1152/ajpcell.00124.2023](https://doi.org/10.1152/ajpcell.00124.2023).
- Meers MP, Henriques T, Lavender CA, McKay DJ, Strahl BD, Duronio RJ, Adelman K, Matera AG. 2017. Histone gene replacement reveals a post-transcriptional role for H3K36 in maintaining metazoan transcriptome fidelity. *Elife*. 6:e23249. doi:[10.7554/eLife.23249](https://doi.org/10.7554/eLife.23249).
- Meers MP, Leatham-Jensen M, Penke TJR, McKay DJ, Duronio RJ, Matera AG. 2018. An animal model for genetic analysis of multi-gene families: cloning and transgenesis of large tandemly repeated histone gene clusters. *Methods Mol Biol*. 1832:309–325. doi:[10.1007/978-1-4939-8663-7_17](https://doi.org/10.1007/978-1-4939-8663-7_17).
- Mohn F, Sienski G, Handler D, Brennecke J. 2014. The rhino-deadlock-cutoff complex licenses noncanonical transcription of dual-strand piRNA clusters in *Drosophila*. *Cell*. 157(6): 1364–1379. doi:[10.1016/j.cell.2014.04.031](https://doi.org/10.1016/j.cell.2014.04.031).
- Muller L, Fulop T, Pawelec G. 2013. Immunosenescence in vertebrates and invertebrates. *Immun Ageing*. 10(1):12. doi:[10.1186/1742-4933-10-12](https://doi.org/10.1186/1742-4933-10-12).
- Naylor RM, Baker DJ, van Deursen JM. 2013. Senescent cells: a novel therapeutic target for aging and age-related diseases. *Clin Pharmacol Ther*. 93(1):105–116. doi:[10.1038/clpt.2012.193](https://doi.org/10.1038/clpt.2012.193).
- Ni Z, Ebata A, Alipanahramandi E, Lee SS. 2012. Two SET domain containing genes link epigenetic changes and aging in *Caenorhabditis elegans*. *Aging Cell*. 11(2):315–325. doi:[10.1111/j.1474-9726.2011.00785.x](https://doi.org/10.1111/j.1474-9726.2011.00785.x).
- Ochoa Thomas E, Zuniga G, Sun W, Frost B. 2020. Awakening the dark side: retrotransposon activation in neurodegenerative disorders. *Curr Opin Neurobiol*. 61:65–72. doi:[10.1016/j.comb.2020.01.012](https://doi.org/10.1016/j.comb.2020.01.012).
- Pardue ML, Rashkova S, Casacuberta E, DeBaryshe PG, George JA, Traverse KL. 2005. Two retrotransposons maintain telomeres in *Drosophila*. *Chromosome Res*. 13(5):443–453. doi:[10.1007/s10577-005-0993-6](https://doi.org/10.1007/s10577-005-0993-6).
- Peleg S, Feller C, Forne I, Schiller E, Sevin DC, Schauer T, Regnard C, Straub T, Prestel M, Klima C, et al. 2016a. Life span extension by targeting a link between metabolism and histone acetylation in *Drosophila*. *EMBO Rep*. 17(3):455–469. doi:[10.15252/embr.201541132](https://doi.org/10.15252/embr.201541132).
- Peleg S, Feller C, Ladurner AG, Imhof A. 2016b. The metabolic impact on histone acetylation and transcription in ageing. *Trends Biochem Sci*. 41(8):700–711. doi:[10.1016/j.tibs.2016.05.008](https://doi.org/10.1016/j.tibs.2016.05.008).
- Penke TJR, McKay DJ, Strahl BD, Matera AG, Duronio RJ. 2018. Functional redundancy of variant and canonical histone H3 lysine 9 modification in *Drosophila*. *Genetics*. 208(1):229–244. doi:[10.1534/genetics.117.300480](https://doi.org/10.1534/genetics.117.300480).
- Piazzesi A, Papic D, Bertan F, Salomoni P, Nicotera P, Nicotera P, Bano D. 2016. Replication-independent histone variant H3.3 controls

- animal lifespan through the regulation of pro-longevity transcriptional programs. *Cell Rep.* 17(4):987–996. doi:10.1016/j.celrep.2016.09.074.
- Pu M, Ni Z, Wang M, Wang X, Wood JG, Helfand SL, Yu H, Lee SS. 2015. Trimethylation of Lys36 on H3 restricts gene expression change during aging and impacts life span. *Genes Dev.* 29(7):718–731. doi:10.1101/gad.254144.114.
- Quinlan AR, Hall IM. 2010. BEDTools: a flexible suite of utilities for comparing genomic features. *Bioinformatics.* 26(6):841–842. doi:10.1093/bioinformatics/btq033.
- Ransom M, Dennehey BK, Tyler JK. 2010. Chaperoning histones during DNA replication and repair. *Cell.* 140(2):183–195. doi:10.1016/j.cell.2010.01.004.
- Reimand J, Kull M, Peterson H, Hansen J, Vilo J. 2007. g:Profiler—a web-based toolset for functional profiling of gene lists from large-scale experiments. *Nucleic Acids Res.* 35(suppl_2):W193–W200. doi:10.1093/nar/gkm226.
- Rothbart SB, Strahl BD. 2014. Interpreting the language of histone and DNA modifications. *Biochim Biophys Acta.* 1839(8):627–643. doi:10.1016/j.bbagr.2014.03.001.
- Ryu JH, Kim SH, Lee HY, Bai JY, Nam YD, Bae J-W, Lee DG, Shin SC, Ha E-M, Lee W-J. 2008. Innate immune homeostasis by the homeobox gene caudal and commensal-gut mutualism in *Drosophila*. *Science.* 319(5864):777–782. doi:10.1126/science.1149357.
- Ryu JH, Nam KB, Oh CT, Nam HJ, Kim SH, Yoon J-H, Seong J-K, Yoo M-A, Jang I-H, Brey PT, et al. 2004. The homeobox gene caudal regulates constitutive local expression of antimicrobial peptide genes in *Drosophila epithelia*. *Mol Cell Biol.* 24(1):172–185. doi:10.1128/MCB.24.1.172-185.2004.
- Sadic D, Schmidt K, Groh S, Kondofersky I, Ellwart J, Fuchs C, Theis FJ, Schotta G. 2015. Atrx promotes heterochromatin formation at retrotransposons. *EMBO Rep.* 16(7):836–850. doi:10.15252/embr.201439937.
- Sakai A, Schwartz BE, Goldstein S, Ahmad K. 2009. Transcriptional and developmental functions of the H3.3 histone variant in *Drosophila*. *Curr Biol.* 19(21):1816–1820. doi:10.1016/j.cub.2009.09.021.
- Salzler HR, Vandadi V, McMichael BD, Brown JC, Boerma SA, Leatham-Jensen MP, Adams KM, Meers MP, Simon JM, Duronio RJ, et al. 2023. Distinct roles for canonical and variant histone H3 lysine-36 in polycomb silencing. *Sci Adv.* 9(9):eadf2451. doi:10.1126/sciadv.adf2451.
- Savitsky M, Kwon D, Georgiev P, Kalmykova A, Gvozdev V. 2006. Telomere elongation is under the control of the RNAi-based mechanism in the *Drosophila* germline. *Genes Dev.* 20(3):345–354. doi:10.1101/gad.370206.
- Schoberleitner I, Bauer I, Huang A, Andreyeva EN, Sebald J, Pascher K, Rieder D, Brunner M, Podhraski V, Oemer G, et al. 2021. CHD1 controls H3.3 incorporation in adult brain chromatin to maintain metabolic homeostasis and normal lifespan. *Cell Rep.* 37(1):109769. doi:10.1016/j.celrep.2021.109769.
- Sen P, Dang W, Donahue G, Dai J, Dorsey J, Cao X, Liu W, Cao K, Perry R, Lee JY, et al. 2015. H3k36 methylation promotes longevity by enhancing transcriptional fidelity. *Genes Dev.* 29(13):1362–1376. doi:10.1101/gad.263707.115.
- Sen P, Shah PP, Nativio R, Berger SL. 2016. Epigenetic mechanisms of longevity and aging. *Cell.* 166(4):822–839. doi:10.1016/j.cell.2016.07.050.
- Seong CS, Varela-Ramirez A, Tang X, Anchondo B, Magallanes D, Aguilera RJ. 2014. Cloning and characterization of a novel *Drosophila* stress induced DNase. *PLoS One.* 9(8):e103564. doi:10.1371/journal.pone.0103564.
- Siebold AP, Banerjee R, Tie F, Kiss DL, Moskowitz J, Harte PJ. 2010. Polycomb repressive Complex 2 and Trithorax modulate *Drosophila* longevity and stress resistance. *Proc Natl Acad Sci U S A.* 107(1):169–174. doi:10.1073/pnas.0907739107.
- Silva-Sousa R, Casacuberta E. 2013. The JIL-1 kinase affects telomere expression in the different telomere domains of *Drosophila*. *PLoS One.* 8(11):e81543. doi:10.1371/journal.pone.0081543.
- Silva-Sousa R, Lopez-Panades E, Pineyro D, Casacuberta E. 2012. The chromosomal proteins JIL-1 and Z4/Putzig regulate the telomeric chromatin in *Drosophila melanogaster*. *PLoS Genet.* 8(12):e1003153. doi:10.1371/journal.pgen.1003153.
- Talbert PB, Henikoff S. 2010. Histone variants—ancient wrap artists of the epigenome. *Nat Rev Mol Cell Biol.* 11(4):264–275. doi:10.1038/nrm2861.
- Udugama M, F MCFT, Chan L, Tang MC, Pickett HA, McGhie JDR, Mayne L, Collas P, Mann JR, Wong LH. 2015. Histone variant H3.3 provides the heterochromatic H3 lysine 9 tri-methylation mark at telomeres. *Nucleic Acids Res.* 43(21):10227–10237. doi:10.1093/nar/gkv847.
- Wallrath LL, Elgin SC. 1995. Position effect variegation in *Drosophila* is associated with an altered chromatin structure. *Genes Dev.* 9(10):1263–1277. doi:10.1101/gad.9.10.1263.
- Wenger A, Biran A, Alcaraz N, Redo-Riveiro A, Sell AC, Krautz R, Flury V, Reverón-Gómez N, Solís-Mezarino V, Völker-Albert M, et al. 2023. Symmetric inheritance of parental histones governs epigenome maintenance and embryonic stem cell identity. *Nat Genet.* 55(9):1567–1578. doi:10.1038/s41588-023-01476-x.
- Wong LH, Ren H, Williams E, McGhie J, Ahn S, Sim M, Tam A, Earle E, Anderson MA, Mann J, et al. 2009. Histone H3.3 incorporation provides a unique and functionally essential telomeric chromatin in embryonic stem cells. *Genome Res.* 19(3):404–414. doi:10.1101/gr.084947.108.
- Wood JG, Hillenmeyer S, Lawrence C, Chang C, Hosier S, Lightfoot W, Mukherjee E, Jiang N, Schorl C, Brodsky AS, et al. 2010. Chromatin remodeling in the aging genome of *Drosophila*. *Aging Cell.* 9(6):971–978. doi:10.1111/j.1474-9726.2010.00624.x.
- Wood JG, Jones BC, Jiang N, Chang C, Hosier S, Wickremesinghe P, Garcia M, Hartnett DA, Burhenn L, Neretti N, et al. 2016. Chromatin-modifying genetic interventions suppress age-associated transposable element activation and extend life span in *Drosophila*. *Proc Natl Acad Sci U S A.* 113(40):11277–11282. doi:10.1073/pnas.1604621113.
- Zhang R, Chen HZ, Liu DP. 2015. The four layers of aging. *Cell Syst.* 1(3):180–186. doi:10.1016/j.cels.2015.09.002.
- Zhang W, Deng H, Bao X, Lerach S, Girton J, Johansen J, Johansen KM. 2006. The JIL-1 histone H3S10 kinase regulates dimethyl H3K9 modifications and heterochromatic spreading in *Drosophila*. *Development.* 133(2):229–235. doi:10.1242/dev.02199.
- Zhang G, Li J, Purkayastha S, Tang Y, Zhang H, Yin Y, Li B, Liu G, Cai D. 2013. Hypothalamic programming of systemic ageing involving IKK-beta, NF-kappaB and GnRH. *Nature.* 497(7448):211–216. doi:10.1038/nature12143.